RAM ROBOTICS AND MECHATRONICS

ENERGY BASED SAFETY FOR PASSIVE ROBOTS PERFORMING ACTIVE INTERACTION TASKS

D. (Daniel) van Dijk

MSC ASSIGNMENT

Committee:
prof. dr. ir. S. Stramigioli
dr. ir. W. Roozing
dr. ir. F. Califano
dr. ir. A.Q.L. Keemink

January, 2022

004RaM2022
Robotics and Mechatronics
EEMathCS
University of Twente
P.O. Box 217
7500 AE Enschede
The Netherlands

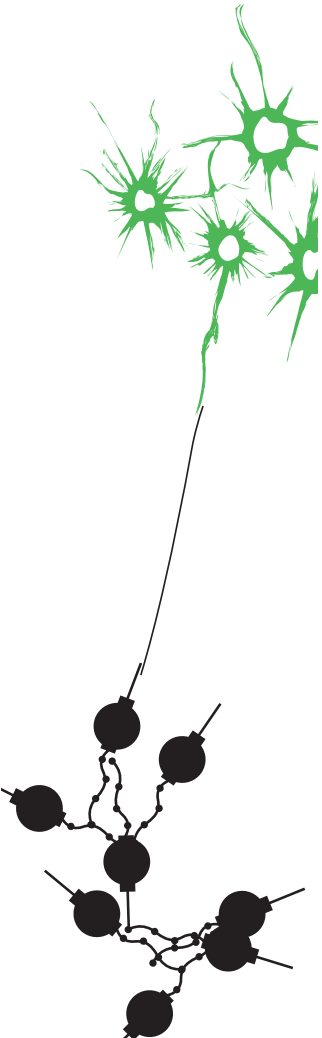

UNIVERSITY OF TWENTE. | TECHMED CENTRE UNIVERSITY OF TWENTE. | DIGITAL SOCIETY INSTITUTE

Abstract

Automatisation is spreading rapidly in all kind of sectors, giving rise to new problems that need solutions. One of those problems is the safe usage of manipulator robots in environments where a human and robot share their workspace. In this thesis, a novel safety-aware control architecture is proposed. This is done by utilising a novel dynamic energy injection protocol using energy tanks, accompanied by compliance based control in case of collisions. Collision experiments on a 7-DoF manipulator show the validity of the proposed control architecture.

Contents

1 Introduction

This master thesis report encompasses the most relevant parts of the work done during the graduation project. In the first chapter the motivation is given for the chosen topic and provides the research question at hand. Chapter 2 will provide the reader with the necessary background material required for understanding the decisions made during the thesis. The main work of the thesis will be presented in the form of a conference paper, which is shown in Chapter 3. Finally, we reflect on the work done during the graduation project in Chapter 4.

This project is a partial extension of the work done in "Energy-aware adaptive impedance control using offline task-based optimization" [1]. The thesis will focus on experimentally validating some of the key contributions made in [1]. On top of that, in this work some novel key contributions are made towards manipulator safety in a shared human-robot environment.

1.1 Motivation: Interaction control with collaborative robots

Automatisation is continuously expanding and shows no sign of stopping. Recent advances in automatisation are in the field of collaborative robots (cobots), where robots have to operate near or with a human. Applications for cobots can be found in care robots for the elderly or disabled, where assisting with dressing, carrying, washing etc. requires large strong robots to perform these tasks, while also having to interact in a safe manner [2]. Additionally, applications can be found in warehousing, logistics or service robots for domestic applications [3]. Although the industries of these applications are diverse, they all share the same requirement of safe human-robot interaction in a shared workspace. Therefore, these robots needs to be carefully designed to mitigate safety hazards.

Safe human-robot interaction in a shared environment is (partly) a problem of 'control', where control is the answer to the question *"How can we make the robot behave in a desired way?"*. Conventional control theories such as position/velocity (motion) or force/torque control are not suitable for interaction between robot and environment. Therefore, most recent works concerning robot interaction, use a form of impedance or admittance control [4–7]. The impedance control framework forms the basis for the thesis and will be elaborated in the next section.

Robots have a wide range of use. Therefore, it is necessary to specify the scope in which the robots will be used in this assignment. Robots working together with humans can be classified in three broad categories [3]:

- *Supportive:* The robot is not integral to the central performance of the task, but instead provides the human with the tools, materials, and information to help the human with it's task. For example, tour guide robots, shopping assisting robots or domestic household robots. In this scenario physical human-robot interaction is infrequent and only for a short amount of time, i.e. handing objects.
- *Collaborative:* The human and robot both work on the task, with the human and robot separately performing their task, but with more frequent interaction through turn-taking or exchange of objects. In this scenario the robot completes the tasks not suited for humans e.g. repetitive, high-force, toxic or precision tasks. The interaction between human and robot in this scenario will only last for a short amount of time and is generally planned.

- *Cooperative:* The robot acts independently from the human and interaction is no longer planned. The human and robot work together in both direct and indirect physical contact for a undefined amount of time. Examples are, lifting and carrying, kinesthetic teaching, material handling and rehabilitation therapy.

Both in supportive and collaborative interactions the human and robot share the same workspace and interactions are planned and short in time. Cooperative interaction requires unplanned interaction and is therefore not a suitable form of interaction for our control technique, which requires information about the task to be available, in other words *planned* interaction. In conclusion, the scope of this work will be limited to humans and robots working in either a supportive or collaborative setting.

1.2 Previous Work

This section aims to provide the reader with a basic understanding of some key concepts that have been introduced in other works.

1.2.1 Impedance Control and Energy Shaping

Impedance control was first introduced in a threefold paper by Hogan [8–10]. Impedance can be domain independently defined via the power conjugated variables *effort* and *flow* described by:

$$Z = \frac{e}{f} \tag{1.1}$$

In case of the mechanical domain this would mean the force divided by the velocity. The goal in Impedance control is to achieve a certain relation between effort and flow, such that the energy of the total system is shaped in such a way that there is an energy-minimum at the desired state. As opposed to classical control, such as motion control or torque/force control, where a reference is given in the form of the respective control variable, the goal is to follow this reference as accurately as possible. A consequence of impedance control is that the system will converge to the desired state if there is dissipation present, as such systems always converge to the state of an energy minimum. This makes it a more suitable method for interaction control with respect to the classical control methods. This method is usually referred to as 'Energy Shaping'.

Example 1: Joint space impedance control of an arbitrary manipulator

Consider the standard equation describing an arbitrary degree-of-freedom (DoF) manipulator.

$$\boldsymbol{M}(\boldsymbol{q})\ddot{\boldsymbol{q}} + \boldsymbol{C}(\boldsymbol{q},\dot{\boldsymbol{q}})\dot{\boldsymbol{q}} + \boldsymbol{G}(\boldsymbol{q}) = \boldsymbol{\tau}^\top \tag{1.2}$$

Where $\boldsymbol{M}(\boldsymbol{q})$ is the inertia matrix, $\boldsymbol{C}(\boldsymbol{q},\dot{\boldsymbol{q}})$ contains the Coriolis and centrifugal terms $\boldsymbol{G}(\boldsymbol{q})$ is the torque caused by gravity. $\boldsymbol{\tau}$ represent all the input torques. Assume that we can chose $\boldsymbol{\tau}$ exactly, i.e. there are no external disturbances. We can choose the torque such that we shape the energy potential of the system. We do this by compensating for the gravity term $\boldsymbol{G}(\boldsymbol{q})$, and adding a spring $\boldsymbol{K}$ and damper $\boldsymbol{B}$. The chosen control torque becomes,

$$\boldsymbol{\tau} = \boldsymbol{G}(\boldsymbol{q}) + \frac{\partial(\frac{1}{2}(\boldsymbol{q}^* - \boldsymbol{q})^\top \boldsymbol{K}(\boldsymbol{q}^* - \boldsymbol{q}))}{\partial \boldsymbol{q}} - \boldsymbol{B}\dot{\boldsymbol{q}}, \tag{1.3}$$

where $\boldsymbol{q}^*$ is the desired state. Assuming perfect compensation of the gravity term, the total energy potential of the system becomes,

$$V = \frac{1}{2}(\boldsymbol{q}^* - \boldsymbol{q})^\top \boldsymbol{K}(\boldsymbol{q}^* - \boldsymbol{q}) \tag{1.4}$$

Since the damper is dissipating energy the system will converge to the lowest possible energy state, which is when $\boldsymbol{q} = \boldsymbol{q}^*$.

Next to joint space impedance control it is also possible to control the manipulator in Cartesian space, which is more suitable for the way tasks are usually defined. This will be further discussed in Chapter 2.

1.2.2 Safety in Robotics

When operating heavy manipulators used in industry there are numerous safety hazards in the form of collisions, clamped configurations or soft-tissue injuries. These safety hazards can at least be partly eliminated by mechanical design [11], but in case this is not possible, sufficient or desirable additional measures have to be taken. For example, it is possible to use external sensors to detect objects before collision [12, 13] and exploit information on object location and orientation to ensure safe behaviour [14]. However, this comes with the significant downside of having to use additional sensors, which are expensive and have to be incorporated in the design. Therefore, a lot of research is done on finding a suitable control framework in which safe operation can be guaranteed by using only a set of standard sensors, such as joint encoders and torque sensors.

Safety in robotics can be split into two categories: pre-impact and post-impact. Pre-impact safety concerns itself with putting constraints on the robot movement to limit the severity of injury in case of collision. For example, limiting the impact force [15] can prevent injuries such as bone fracture or internal bleeding. Another approach is to put limits on the power and energy of the system [4, 16–20]. Post-impact safety consists of the detection of the collision and the reaction to it. There are various possibilities for detecting collisions without the use of external sensors. For instance, in [21] the motor current is used for collision detection, while in [22] a torque disturbance observer is proposed. Another possibility is to look at the generalised momentum [23] or integrate energy tanks in the fault detection scheme [24].

Details on what has been done in the field of safety for robotic manipulators will be elaborated further in chapter 2.

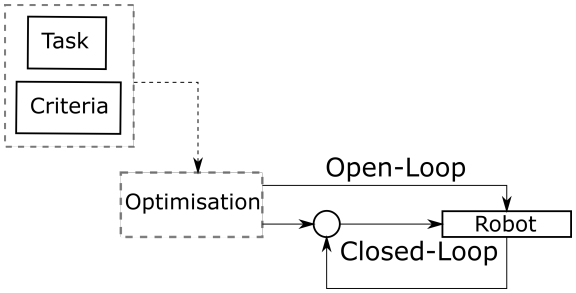

Figure 1.1: An example control scheme with a task-based open-loop control action, supplemented with a closed loop control action.

1.2.3 Optimisation

In Section 1.2.1, example 1, it is shown how a basic impedance controller can be implemented, but the question remains: how are the impedance parameters, $\boldsymbol{K}$ and $\boldsymbol{B}$, chosen? In literature a popular topic is that of a variable impedance. This can be done by varying $\boldsymbol{K}$ either in time [7] or space [25] or a combination of the two. An impedance that is only variable in time is called open-loop control, as it does not take into consideration any unexpected changes with respect to the system model. On the other hand a variable impedance in space or a combination of space and time requires information of the manipulator configuration, which is called closed-loop control. In [26] it was reasoned that it is beneficial for robot safety to have minimal feedback. Therefore, an example control scheme as given in Fig. 1.1 could be used to make the robot behaviour safer.

In this thesis we build on the strategy proposed in [1], where a task-based optimisation strategy is used to construct an open-loop control action. The open-loop control action is supported with a closed-loop control action to adjust for small discrepancies from the nominal case. The optimal variable impedance can be chosen based on the following criteria:

- *Performance:* For each deviation from the planned trajectory or positions an increase in cost is defined. The performance cost can be split in multiple terms, dependent on the objective. Examples of performance objectives can be to minimise the tracking error or the error at the final time.
- *Energy efficiency:* Energy efficiency can be expressed in a form of metabolic cost, which is defined as the energy spend during the task. The metabolic cost can be partly attributed due to dissipation in the electrical part of the motors, and the mechanical power.
- *Stiffness:* For safety reasons it is desired to minimise the interaction energy, which is equivalent to minimising the stiffness of the impedance control loop.

Hence, an optimisation problem can be constructed that minimizes the sum of the weighted costs attributed to each of the above mentioned criteria. Choosing the damper $\boldsymbol{B}$ can be done in a similar fashion or by making it dependent on $\boldsymbol{K}$.

1.3 Problem Description

1.3.1 General problem

In impedance control a hot topic remains in how to choose the impedance parameters. Previous work has shown that both bio-mimetic and performance metrics can be cast into an optimisation problem to create interpretable optimal values for the impedance parameters [1]. However, these results have only been tested in simulation and require experimental validation. Additionally, the method as proposed in [1] does not result in a control strategy that is

safe for humans and robots to operate in a shared workspace. This gives rise to a need for a supplementary safety layer.

1.3.2 Project scope

The control strategy as presented in [1] consists of a task-based open-loop optimisation in an impedance control framework, supplemented with passivity layer in the form of energy tanks and a closed-loop impedance controller to compensate for model variations and external disturbances. Next to that, an iterative feed-forward adaption law was incorporated to update the open-loop control action and energy budgets after each iteration. However, due to the limited amount of time available it is chosen to leave iterative feed-forward adaption law out of the assignment.

The control strategy has shown promising results in simulation, but experimental validation was missing. Therefore, the following research questions are proposed:

"Is it achievable to implement the control strategy on a commonly used manipulator? Does it still have the same benefits over conventional control as shown in the simulation results?"

Next to that, there are some concerns about the safety of the control strategy. Hence, an additional research question is put forth:

"Is the control strategy presented safe for human-robot collaboration in a shared workspace? What steps are necessary to make the control strategy safe for humans and robots in a shared workspace?"

1.4 Contribution

The major contributions of the thesis will be twofold:

1. Experimental validation of a control strategy based on a time-varying task-based optimisation in a Cartesian impedance control framework and a closed-loop task-free impedance controller.
2. A safety layer exploiting the well known concepts of energy tanks, which is able to accurately detect and react to unexpected collisions.

1.5 Approach

1.5.1 Setup

The robot of choice is the 7-DoF Franka Emika Panda robot or 'Franka', which can be seen in Fig. 1.2. The robot is chosen, mainly because of its availability, but also because of the relatively easy interface, as communication can be done via the Robotic Operating System (ROS). This communication interface is shown in Fig. 1.3.

1.5.2 Control structure: task-based and task-free

The control structure will consist of a optimised open-loop control action in a Cartesian space variable impedance framework, called the task-based control term. Additionally, we provide a closed-loop control action to compensate for model deviations or small disturbances, which is called the task-free control term. See Fig. 1.1 for a schematic representation of this architecture.

Figure 1.2: The Franka Emika Panda robot. It is a 7-DoF manipulator with a reach of 0.855 m and can carry a payload up to 3 kg. Besides that it is equipped with link-side torque sensors in each joint and an independently controllable gripper with a maximum width of 0.080 m.

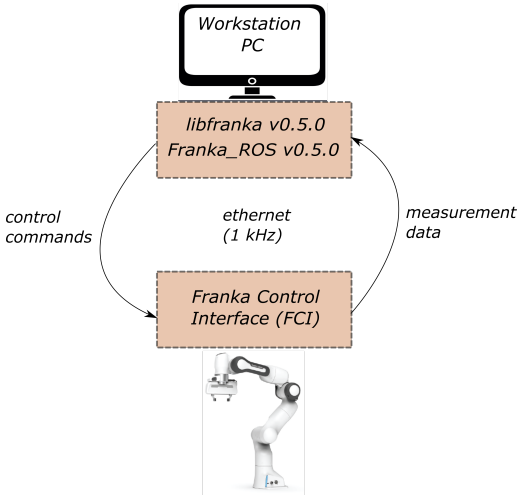

Figure 1.3: Schematic overview of the communication between workstation and robot.

1.5.3 Optimisation

An optimisation algorithm will be constructed to be able to find optimal values for the impedance parameters of the task-based control action. Due to the exceptional performance of humans in every day tasks such as grabbing, moving and lifting it is chosen to approach the optimisation problem for a bio-mimetic perspective. The optimisation problem is continuous in time, however, due to practical limitations we seek the solution of the optimisation to be a set of finite parameters.

1.5.4 Safety Layer

Since we will be using non-passive control actions, as we want to do active work, the system will be non-passive. Energy tanks are an elegant way to recover passivity. However, passivity does not necessarily mean safety [4]. The energy tank approach fits very well within the task-based paradigm, as for a pre-determined task we can determine the nominal energy spent to complete the task, which in turn can be used to fill the tanks accordingly. However, for some tasks this may be a significant amount of energy, which can lead to unsafe behaviour because there is no limit on the speed at which the energy can be extracted from the tank. Therefore, we utilise a novel dynamic energy injection strategy that is based on the strategy proposed in [1].

1.5.5 Procedure and validation

The methods will be validated by doing experiments on a real-life manipulator. A benchmark experiment for industrial robotics is a peg-in-hole task. To get acquainted with the material from [1] a case study is performed. This case study aims to incorporate the various aspects of the control strategy and the safety layer in a simple double pendulum model, such that a basic understanding of the control architecture is obtained. Additionally, this model would provide us with the opportunity to identify problems in the strategy early on. This model will be built in MATLAB 2020b and Simulink. Finally, the control strategy and safety layer need to be incorporated on the Franka, which is provided with a control interface via the ROS (Robotic Operating System) package *libfranka*. The libfranka library consists of various example controllers made in C++, therefore, the programming language of choice will also be C++.

1.6 Report Structure

The thesis report consists of four chapters, of which this introductory chapter was the first. This is followed by a background chapter which will provide more detail on what has been done in previous work and provides the author with the various options available for the safety layer. A choice will be made on the final control strategy and safety layer and be used for the experiments on the Franka manipulator, which will be processed into a paper given in Chapter 3. Lastly, there will be a reflection on the work done during the graduation project. In this chapter we will look back to our problem statement from this section and provide some conclusions for it.

2 Background

Industrial robotic arms are frequently denoted as 'manipulator', as the robotic arm manipulates the environment by performing tasks. The Franka Emika Panda, which will be used for the final experiments, is a redundant manipulator with 7 degrees of freedom. With a total mass of 18 kg and 2 $m\,s^{-1}$ end effector speed it poses a potential safety hazard.

This chapter is divided in two main sections. In the first section we will outline the relevant safety risks while dealing with such a manipulator, and present solutions to these safety risks found in literature. For the second section we provide some theoretical background on safety relevant aspects that we might have to deal with when ensuring safe manipulator behaviour.

2.1 Safety

2.1.1 Safety concerns in a manipulator

There are numerous safety concerns when working with manipulators. A graphical summary is given in Fig. 2.1. The unconstrained and constrained impact scenarios are the main scenarios that will be dealt with in this work.

To determine all safety relevant metrics, a safety analysis is done for an arbitrary manipulator. This consists of the following steps:

1. Risk assessment
2. Risk elimination and reduction
3. Quantitative norms

2.1.1.1 Risk assessment

Identifying the safety risks for the manipulator can be done with the help of the two main scenarios; *constrained* and *unconstrained* impact. In case of a constrained impact, the human is locked between the manipulator and a static object. In case of unconstrained impact the human is free to move in any direction. Other scenarios, such as the clamping or secondary impact scenarios, are not incorporated in this work due to the unlikeliness of occurrence or lack of controllability in the specific situation.

The following risks can be identified when working with a manipulator [27]:

- Blunt Impact
  - Fracture
  - Internal bleeding
- Soft Tissue
  - Abrasion
  - Contusion
  - Stab wounds
  - Laceration

Blunt Impact For blunt impact collisions fractures and internal bleeding are the main concerns. Especially when colliding with delicate parts of the human body such as the neck or head. Blunt impact collisions require slightly different safety measures depending on whether the human is constrained or unconstrained. In case of constrained impact it is very important the the robot does not attempt to move any further and becomes compliant as soon as possible, such that the human can remove the robot from contact. In case of unconstrained impact

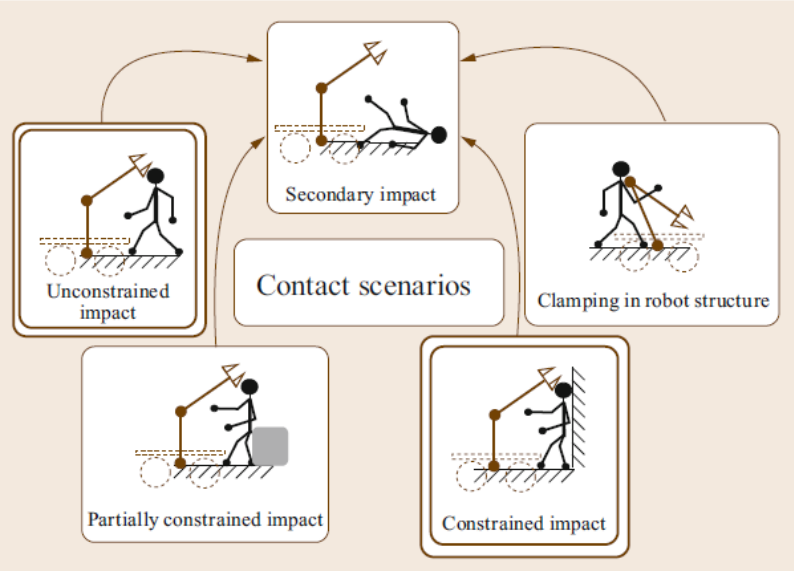

Figure 2.1: Contact scenarios for human-robot collision, from [3]

the initial impact force is the determining factor for the resulting injury, as the risk of sustained pressure is much lower with respect to the constrained scenario.

Soft Tissue

- **Abrasion:** Abrasions are mainly caused by tangential motions of corners and sharp edges along the human skin and an affecting energy of $E = 100\,\mathrm{J}$ is already enough to cause such injury [28].
- **Contusion (bruises, crushes):** Contusions are a matter of impact density. Typical high-danger parts of the human body are the scalp on kneecaps due to their osseous basis. Tissue injury occurs at an energy density of $\epsilon_A > 2.52 \times 10^4\,\mathrm{J\,m^{-2}}$ [28].
- **Stab wounds:** Stab wounds can occur if the chosen end-effector tool is a sharp object such as a knife, scissor or scalpel. Concerning stab wounds a useful metric for injury is penetration force, as strain is no appropriate measure due to the small contact area. Tolerance to penetration force depends heavily on the layers of clothing and range from 76 N for uncovered skin to 173 N for three layers of typical clothing. For common tools such as scissors or kitchen knifes the value are between $60 - 76\,\mathrm{N}$ [27].
- **Laceration (cuts, gashes, contused wounds):** At low velocities of $0.25\,\mathrm{m\,s^{-1}}$ no injuries are observed, while at $0.8\,\mathrm{m\,s^{-1}}$ large and deep lacerations can be caused by common sharp tools [27].

2.1.1.2 Risk elimination and reduction

Blunt Impact The blunt impact injury can be reduced by putting limits on the allowable impact force, which is dependent on the Jacobian, inertia matrix and velocity of the robot for a collision with a stationary rigid object, as will be shown in Section 2.2. To solve the issue of blunt impact in case of a constrained scenario, e.g. a sustained force, there is need for a reliable collision detection and reaction strategy. This will be further discussed in Section 2.1.2 and Section 2.1.3.

Soft Tissue For the soft tissue injury types it is assumed that the end-effector tool is not sharp. Therefore, only abrasions and contusions have to be taken into consideration. The abrasion type injury can be prevented by a sufficiently accurate collision detection and reaction strategy, as abrasions require sustained tangential motion along the skin. Contusions can be prevented by limiting the kinetic energy of each joint or other point-of-interest, as the transferred energy

to the collided object can be limited by kinetic energy.

The risk elimination and reduction scheme can be found in Fig. 2.2.

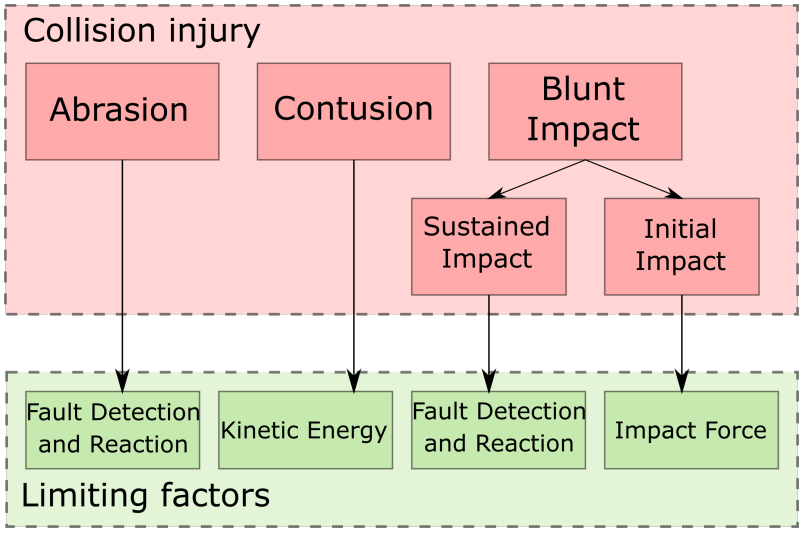

Figure 2.2: Safety tree showing each injury risk and the factor that limits the severity of the injury.

2.1.1.3 Quantative norms

Blunt Impact A quantitative norm frequently used in the automotive industry is the Head Injury Criterion (HIC). However, due to the relatively low operating velocities of manipulator robots, even the heaviest robots are deemed safe according to the HIC [29]. A more relevant metric for robots has come up in [30], namely, the Head Impact Power (HIP). These power (and energy) limits are given in (2.1) and (2.2).

$$P_{\text{limit}} \approx 5\,\text{kW} \tag{2.1}$$

$$E_{\text{limit}} = 30\,\text{J} \tag{2.2}$$

The power limit is chosen such that their is 'only' a 5% chance at concussion in case of impact. The energy limit is chosen for neck fracture, as the neck has the lowest force tolerance of all body parts [18]. However, these limits are taken at the boundary of very serious injury, namely neck fracture. In [3] it was attempted to find a correlation with pain, which sets the limits for energy as,

$$E_{\text{limit}} = 12.2\,\text{J} \tag{2.3}$$

We take the more conservative limit of (2.3). Concerning the impact force limit, pain experiments with a human has shown that the impact force limit can be taken as given in (2.4) [3].

$$F_{\text{limit}} = 272.2N \tag{2.4}$$

Soft Tissue Quantitative norms for soft tissue injuries are specified in [28]. This states that the limit for energy density before a contusion type injury will occur is,

$$\epsilon_A = 2.52 \times 10^4\,\text{J}\,\text{m}^{-2} \tag{2.5}$$

An overview of the safety limits is given in table 2.1.

	Limit	Unit	Source
Kinetic Energy	12.2	[J]	[3]
Power	5000	[W]	[30]
Force	272.2	[N]	[3]
Energy Density	2.52×10^4	[$\mathrm{J\,m^{-2}}$]	[28]

Table 2.1: Safety Limits for an arbitrary manipulator

2.1.2 Fault detection

Fault detection in the scope of this work refers to substantial deviations from the planned task. Fault detection can be used to detect unplanned collisions with an object, and more importantly a human. The detection of human-robot collision is a critical part in designing a safety protocol for human-friendly robot control. It is possible to use external sensors [31] for collision detection. However, the use of external sensors comes at an added costs and it is not always possible to have external sensors on a manipulator. Other forms of collision detection use the motor current [21], torque disturbance observer [22] or generalised momentum [23]. On top of these methods, it is possible to integrate energy tanks in the fault detection scheme. Where an empty tank would result in a possible collision detected or some other faulty behaviour [24]. Additionally, the Franka manipulator has its own collision detection scheme. The user of is able to set an external force in [N] which the Franka will register as a collision.

2.1.3 Reaction Strategy

Once the robot has detect faulty behaviour, e.g. collided with a human, an adequate reaction strategy needs to be performed. Possible reaction strategies are [3]:

- **Stop Robot:** Stop the robot using a braking strategy.
- **Torque Control with Gravity Compensation:** The control mode is switched to a compliance-based controller that ignores previous task trajectory. Gravity compensation is the only torque supplied by the actuators to make the robot as compliant as possible from the collided object point of view.
- **Torque Reflex:** This strategy extends the torque control-based strategy by taken into account the external torque measurement. Where the robot will move in the opposite direction of the measured external torque and thus moves away from the safety hazard.
- **Admittance Reflex:** Reference trajectory modification via admittance-type strategy that uses the external torque. This scheme requires no control switching and the robot quickly drives away from the external torque source and decreases the contact forces until they decay to zero.

Whichever strategy is chosen, stopping the robot will always be the first step after fault detection. This strategy can be supplemented with either of the three other strategies.
The breaking strategy for stopping the robot can be chosen in different ways. One way can be to disregard the planned trajectory and place the desired position at its current position. However, this would result in a stiff robot. Another option is to dissipate the kinetic energy by enabling a high damping on the joint velocities and setting the stiffness in the impedance controller to 0.

2.1.4 Points of Interest

In a manipulator, several links can be moving simultaneously to reach a desired configuration. Therefore, it is not only necessary to evaluate safety for the end-effector, as done in [32], but also for other points of interests (POI). These POI are to be evaluated for safety when attempting to find a suitable control. The POI are spread out over the manipulator, such that the safety of the motion can be evaluated for multiple points along the manipulator.

2.1.5 Conclusion

This section has provided an overview of what has been done in the field of safety concerning robotic manipulators. In Fig. 2.2 the injury prevention tree was given. This shows that there is no need for the power limit as given in table 2.1, as the impact force and kinetic energy limits are sufficient. Additionally, it is necessary to be able to reliably and quickly detect collisions and react adequately to it.

2.2 Theoretical Background

2.2.1 Real-time determination of safety values

In the previous section it was shown that safety in robotics is often associated with either maximum impact force or transferred energy. Therefore, it is necessary to be able to determine these two values during operation, such that they can be incorporated in a safety protocol. It is assumed that the joint positions, inertial information and Jacobian are all available at a sufficient rate and accuracy.

2.2.1.1 Impact Force

One of the most obvious risks for safety is the impact force, that is the force at which a point on the robot collides with the human. Determining the impact force is not trivial, but the equation for the impact force, in case of a collision with a rigid object, can be found in (2.6) for a stationary rigid object [33].

$$\hat{f} = \frac{-(1+e)v^\top n}{n^\top J_\mathrm{p}(\theta) M^{-1}(\theta) J_\mathrm{p}^\top n} \tag{2.6}$$

Where $v \in \mathbb{R}$ is the velocity of the mechanical system at the point of impact. $\theta \in \mathbb{R}$ are the joint angles. $J_\mathrm{p}(\theta)$ is the Jacobian at the point of impact and M is the nxn inertia matrix, n is the contact normal. e is a constant denoting the type of collision taking place where $0 < e < 1$, 0 is for purely plastic collision and 1 is for purely elastic collision. Equation (2.6) was modified by [15] such that friction is taken into consideration. The result can be found in (2.7).

$$\hat{f} = \frac{(1+e)s_\mathrm{v}^3}{v^\top J_\mathrm{p}(\theta) M^{-1}(\theta) J_\mathrm{p}^\top v} \tag{2.7}$$

Where $s_v = |v|$. This modification removes the wedge effect and makes for a more realistic behaviour of the effective impact force.

Equations (2.6) and (2.7) show the resulting impact force in case of collision between the robot and a stationary rigid object. Hence, these equations are not suitable for determining the impact force in case of human-robot interaction.

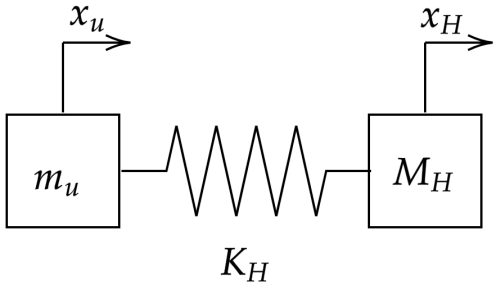

Figure 2.3: Human-robot collision simplified in a mass-spring-mass model

Human-robot collision can be simplified to a mass-spring-mass model, see Fig. 2.3. The initial maximum impact force can than be described by: [3].

$$F_{\text{ext}}^{max} = \sqrt{\frac{m_{\text{u}} M_{\text{H}}}{m_{\text{u}} + M_{\text{H}}}} \sqrt{K_{\text{H}}} \dot{x}_{\text{re}}^{0} \tag{2.8}$$

Where M_{H} is the reflected inertia of the human, K_{H} is the contact stiffness (as the Franka is a rigid robot this is mainly the effective stiffness of the human contact area), m_{u} is the effective mass of the robot acting in the instantaneous collision direction and x_{re}^{0} is the relative impact velocity between human and robot. Note that this is a significant simplification to model a very difficult interaction. Usually both the human and the robot are not free floating objects, which complicates the situation a lot. However, modelling such a difficult interaction is out of the scope of this work.

2.2.1.2 Transferred Energy

Energy becomes a safety relevant entity due to the transferred energy between robot and human. Therefore, it is necessary to be able to know how the transferred energy can be determined. This has been done in [17], with the resulting equation (2.9).

$$\Delta T = \frac{1}{2} \frac{m_{\text{H}}}{1 + \frac{m_{\text{H}}}{m_{\text{u}}}} \dot{x}_{\mathbf{n}}^{2} \tag{2.9}$$

Where m_u is the reflected mass of the robot in the collision point along direction $\mathbf{n}$, m_H is the equivalent mass of the human in the point of collision and $\dot{x}_{\mathbf{n}}$ is the velocity of the robot in the direction of the human.

In [17] the approach is to decrease the reflected mass of several points along the robot arm by exploiting the kinematic redundancy of the robot arm, along the directions of potential impacts. By decreasing the reflected mass the total transferred energy during collision is decreased, as can be seen in (2.9).

2.2.2 Passivity and safety

It is required to shortly mention passivity when talking about safety in robotics due to some misconceptions on the influence it has on safe human-robot interaction.

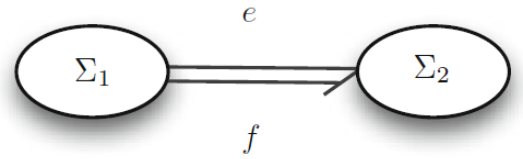

Figure 2.4: Two systems Σ_1 and Σ_2 connected by a power port with power variables effort e and flow f, from [34]

Consider two systems Σ_1 and Σ_2 that are connected by a power port (e,f) as seen in Fig. 2.4. A system is said to be *passive* with respect to the port if the stored energy of Σ_2 is never more than what has been added through the power port plus the initial energy of Σ_2 [4].

In [24] and [35] it is insinuated that a passive system renders a system suitable for human-robot coexistence. There is some truth to it, as a non-passive system can become unsafe due to the possibility of unlimited energy extraction in case of interaction with a passive environment [34]. However, passivity does not guarantee safe behaviour, as passivity does not put a limit on total energy content within the system, nor the rate at which it is released. Section 2.1.1 already

shows that there should be limits on the energy that can be transferred by the system, hence the total energy within the system. Also, passivity has no correlation to the impact force in case of human-robot collision, while impact force has a strong influence on the injury probability in case of human-robot collision [3]. In conclusion, passivity is not a sufficient condition for safe interaction with humans.

2.2.2.1 The control framework and passivity requirement

We base our control framework on the framework presented in [1]. This control scheme is based on a time-varying impedance control. In the following section the difficulty regarding passivity and this control method is shown.

A system is said to be *passive* when the following inequality holds [36],

$$\int_{t_0}^{t_1} \dot{E} dt = E(q(t_1)) - E(q(t_0)) \leq \int_{t_0}^{t_1} y^\top u dt \tag{2.10}$$

Where E is the total energy in the system, q the state, u the input and y the output. If equality holds then the system is said to be *conservative*.

In the following steps it is shown why a variable impedance destroys passivity:

Consider the general equation for describing a robotic arm:

$$\boldsymbol{M}(\boldsymbol{q})\ddot{\boldsymbol{q}} + \boldsymbol{C}(\boldsymbol{q},\dot{\boldsymbol{q}})\dot{\boldsymbol{q}} + \boldsymbol{G}(\boldsymbol{q}) = \boldsymbol{\tau}^\top \tag{2.11}$$

$\boldsymbol{\tau}^\top$ can be split into the controlled torques $\boldsymbol{\tau}_c$ and uncontrolled torques in the form of disturbances $\boldsymbol{\tau}_e$:

$$\boldsymbol{M}(\boldsymbol{q})\ddot{\boldsymbol{q}} + \boldsymbol{C}(\boldsymbol{q},\dot{\boldsymbol{q}})\dot{\boldsymbol{q}} + \boldsymbol{G}(\boldsymbol{q}) = \boldsymbol{\tau_c}^\top + \boldsymbol{\tau_e}^\top \tag{2.12}$$

We need to determine the control torque $\boldsymbol{\tau}_\mathrm{c}$, such that we have an energy minimum at desired state $\boldsymbol{q}^*$. This approach is called energy-shaping. If the system has an energy minimum at a certain state, the system will go to that state, hence we need to shape the energy in such a way that there is an energy minimum at the desired state. Therefore, the resulting $\boldsymbol{\tau}_\mathrm{c}$ is described by:

$$\boldsymbol{\tau}_\mathrm{c} = \hat{\boldsymbol{G}}(\boldsymbol{q}) + \frac{\partial(\frac{1}{2}(\boldsymbol{q}^* - \boldsymbol{q})^\top \boldsymbol{K}(t)(\boldsymbol{q}^* - \boldsymbol{q})}{\partial \boldsymbol{q}}, \tag{2.13}$$

where $\hat{\boldsymbol{G}}(\boldsymbol{q})$ is the estimated influence of gravity on the system. If we assume that the gravity estimation is very accurate, we only have $\boldsymbol{K}(t)$ to shape the energy of the system to have a minimum at the desired state $\boldsymbol{q}^*$. Usually a spring is accompanied by a damper b, the resulting equation describing the model and control framework becomes:

$$\boldsymbol{M}(\boldsymbol{q})\ddot{\boldsymbol{q}} = \boldsymbol{\tau}_\mathrm{e} - \boldsymbol{C}(\boldsymbol{q},\dot{\boldsymbol{q}})\dot{\boldsymbol{q}} + \boldsymbol{K}(t)\tilde{\boldsymbol{q}} - b\dot{\boldsymbol{q}}, \tag{2.14}$$

where $\tilde{\boldsymbol{q}} = \boldsymbol{q}^* - \boldsymbol{q}$.
The total energy of the manipulator is,

$$E = \frac{1}{2}\dot{\boldsymbol{q}}^\top \boldsymbol{M}(\boldsymbol{q})\dot{\boldsymbol{q}} + \frac{1}{2}\tilde{\boldsymbol{q}}^\top \boldsymbol{K}(t)\tilde{\boldsymbol{q}} \tag{2.15}$$

Taking the time derivative to show how the energy changes over time:

$$\dot{E} = \frac{1}{2}\dot{\boldsymbol{q}}^\top \dot{\boldsymbol{M}}(\boldsymbol{q})\dot{\boldsymbol{q}} + \dot{\boldsymbol{q}}^\top \boldsymbol{M}(\boldsymbol{q})\ddot{\boldsymbol{q}} + \tilde{\boldsymbol{q}}^\top \boldsymbol{K}(t)\dot{\tilde{\boldsymbol{q}}} + \frac{1}{2}\tilde{\boldsymbol{q}}^\top \dot{\boldsymbol{K}}(t)\tilde{\boldsymbol{q}} \tag{2.16}$$

Substituting for $\ddot{\boldsymbol{q}}$ and choosing a constant reference ($\dot{\boldsymbol{q}}^* = 0$) gives:

$$\dot{E} = \frac{1}{2}\dot{\boldsymbol{q}}^\top \dot{\boldsymbol{M}}(\boldsymbol{q})\dot{\boldsymbol{q}} + \dot{\boldsymbol{q}}^\top \boldsymbol{\tau}_\mathrm{c} - \dot{\boldsymbol{q}}^\top \boldsymbol{C}(\boldsymbol{q},\dot{\boldsymbol{q}})\dot{\boldsymbol{q}} + \frac{1}{2}\widetilde{\boldsymbol{q}}^\top \dot{\boldsymbol{K}}(t)\widetilde{\boldsymbol{q}} - b\dot{\boldsymbol{q}}^2 \tag{2.17}$$

We can use the following property [37]:

$$\boldsymbol{v}^\top (\dot{\boldsymbol{M}}(\boldsymbol{q}) - 2\boldsymbol{C}(\boldsymbol{q},\dot{\boldsymbol{q}}))\boldsymbol{v} = 0 \tag{2.18}$$

Such that (2.17) becomes:

$$\dot{E} = \dot{\boldsymbol{q}}^\top \boldsymbol{\tau}_\mathrm{c} + \frac{1}{2}\widetilde{\boldsymbol{q}}^\top \dot{\boldsymbol{K}}(t)\widetilde{\boldsymbol{q}} - b\dot{\boldsymbol{q}}^2 \tag{2.19}$$

For a fixed impedance, $\dot{\boldsymbol{K}}(t) = 0$, we can say,

$$\dot{E} = \dot{\boldsymbol{q}}^\top \boldsymbol{\tau}_\mathrm{c} - b\dot{\boldsymbol{q}}^2 \leq \dot{\boldsymbol{q}}^\top \boldsymbol{\tau}_\mathrm{c} \tag{2.20}$$

Hence, the inequality in (2.10) holds. Therefore the system is passive. If there was no damping, i.e. $b = 0$ the system would have been conservative. However, if a variable impedance is used, i.e. $\dot{\boldsymbol{K}}(t) \neq 0$ the energy rate of change becomes,

$$\dot{E} = \dot{\boldsymbol{q}}^\top \boldsymbol{\tau}_\mathrm{c} + \left[\frac{1}{2}\widetilde{\boldsymbol{q}}^\top \dot{\boldsymbol{K}}(t)\widetilde{\boldsymbol{q}} - b\dot{\boldsymbol{q}}^2\right] \tag{2.21}$$

The sign between the square brackets is not defined. Therefore, the system cannot be said to be passive in general. The same could be said if we had a changing reference in time $\dot{\boldsymbol{q}}^* \neq 0$.

A possible solution to this issue is the use of energy tanks. In [18] it is shown for a 1-DoF case where a limited energy supply in the energy tank renders the system passive.

3 Paper

Energy based safety for passive robots performing active interaction tasks

Daniël van Dijk

***Abstract*—In an environment where robots will have to work in close contact with humans, safe human-robot collaboration is critical. In this work, a safety-aware control architecture is constructed along a predefined task. This is done by utilising a novel dynamic energy injection protocol using joint-level energy tanks, accompanied by compliance based control in case of collisions. Collision experiments on a 7-DoF manipulator validate the proposed strategy and show a highly sensitive and reliable safety-aware control architecture.**

***Index terms*— impedance control, optimisation, robot safety, energy tanks, collision detection**

I. Introduction

Recent advances in the field of robotics consider the development of robots that can operate in the same workspace as humans, or even interact with them. These robots are so called collaborative robots (cobots) [1]. Applications of cobots can be found warehousing, logistics or service robots for domestic applications [2, 3]. When operating heavy manipulators used in these areas there are numerous safety hazards in the form of collisions, clamped configurations or soft-tissue injuries. These safety hazards can at least be partly eliminated by mechanical design [4], but in case this is not possible, sufficient or desirable additional measures have to be taken. For example, it is possible to use external sensors such as cameras to detect objects before collision [5, 6] and exploit information on object location and orientation to ensure safe behaviour [7]. Additionally, less invasive sensors such as tactile sensors can be used to detect collisions [8]. However, this comes with the significant downside of having to use additional sensors, which are expensive and have to be incorporated in the design. Therefore, substantial research is done on finding a suitable control framework which is able to detect unsafe conditions using only a set of standard sensors, such as joint encoders and torque sensors. For instance, in [9, 10] disturbance observers are used for collision detection. However, the performance of strategies using disturbance observers is limited by the the accuracy of the robot model.

Safety in robotics can be split into two categories: pre-impact and post-impact. Pre-impact safety concerns itself with putting constraints on the robot movement to limit the severity of injury in case of collision. This can be done by limiting the impact force [11], which prevents injuries such as bone fracture or internal bleeding, or limiting the power or energy of the system [12–17]. Post-impact safety consists of the detection of the collision and the reaction to it.

In this work a novel control architecture is introduced based on the preliminary work presented in [18]. In [19] it was reasoned that it is beneficial for robot safety to have minimal feedback, as this introduces stiff behaviour in order to achieve satisfactory performance. Therefore, the control of a manipulator should consist of a feedforward term and a feedback term. In [18] this is done by constructing an optimised feedforward control action based on a given task, called the task-based control term, and adding a small feedback control action for disturbance rejection, called the task-free control term. Energy tanks were incorporated in the design to guarantee passivity. [18] showed promising results in simulation, but still requires experimental validation. In this work, the task-based control scheme and energy tank architecture from [18] is extended with a safety layer that provides safe manipulator behaviour. This is done by providing a safety metric to the optimisation, including a collision detection protocol, taking advantage of the energy tank architecture, and using an adequate reaction strategy to provide post-impact safety. These contributions are

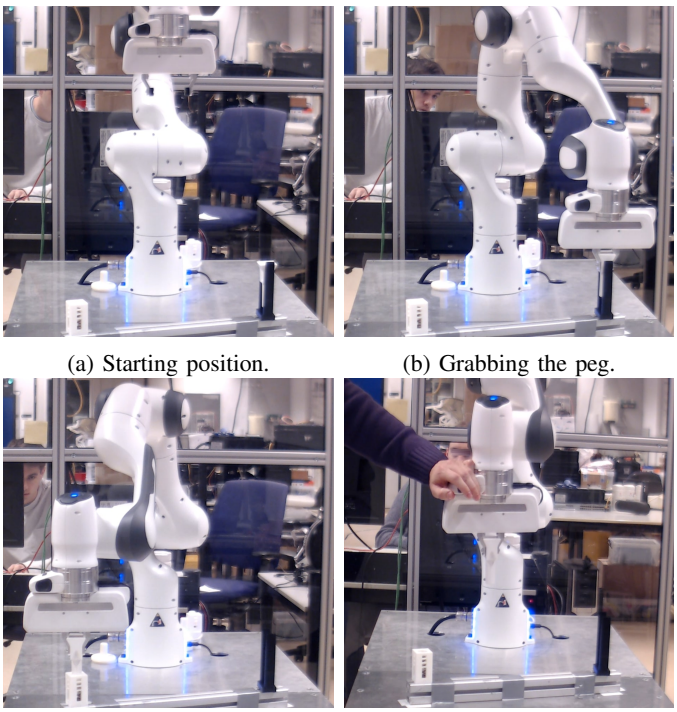

(a) Starting position. (b) Grabbing the peg.

(c) Inserting the peg. (d) Unexpected collision.

Fig. 1: Figs. a-b show the starting position of the task and grabbing of the peg. In Fig. c the peg is successfully inserted and in Fig. d the task could not be completed due to an unexpected collision.

experimentally validated on the 7-DoF Franka Emika Panda manipulator performing a peg-in-hole task, see Fig. 1.

The remainder of this paper is structured as follows. In the next section background material is shown to provide a technical understanding of the used control framework. In Section III the control strategy as introduced in [18] is restated with some small changes. Section IV shows the contributions of this work for manipulator safety. In Section V we outline the experimental setup in which the validation experiments have been performed, followed by Section VI were the results of the experiments are discussed. Conclusions are formulated in Section VII.

II. Background

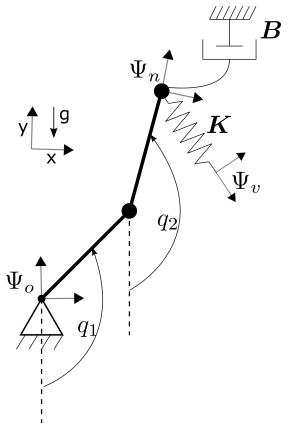

Fig. 2: A manipulator controlled with Cartesian impedance control.

The dynamic model of any manipulator can be described in joint-space coordinates by the following Lagrangian equation [20]:

$$\boldsymbol{M}(\boldsymbol{q})\ddot{\boldsymbol{q}} + \boldsymbol{C}(\boldsymbol{q},\dot{\boldsymbol{q}})\dot{\boldsymbol{q}} + \boldsymbol{G}(\boldsymbol{q}) = \boldsymbol{\tau}^\top + \boldsymbol{\tau}_{\mathrm{e}}^\top, \tag{1}$$

where $\boldsymbol{q}$ are the generalised coordinates, $\boldsymbol{M}(\boldsymbol{q})$ is the inertia matrix, $\boldsymbol{C}(\boldsymbol{q},\dot{\boldsymbol{q}})$ the Coriolis matrix, $\boldsymbol{G}(\boldsymbol{q})$ the torque induced by gravity, $\boldsymbol{\tau}$ are the actuator torques and $\boldsymbol{\tau}_e$ represent the other torques induced by friction or other disturbances. The details on the mathematical framework can be found in [21]. For completeness some key aspects will be restated here.

Consider the arbitrary manipulator as shown in Fig. 2. Frames Ψ_n, Ψ_v and Ψ_o refer to the end-effector, virtual reference and inertial frame respectively. The impedance controller can be generated by means of a virtual spring and damper, with respectively stiffness and damping coefficients $\boldsymbol{K}$ and $\boldsymbol{B}$. The spring pulls the end-effector towards the virtual reference frame, which change of coordinates can be described by the homogeneous transformation matrix:

$$\boldsymbol{H}_n^v = \begin{pmatrix} \boldsymbol{R}_n^v & \boldsymbol{p}_n^v \\ \boldsymbol{0}_{1\times 3} & 1 \end{pmatrix}, \tag{2}$$

where $\boldsymbol{R}_n^v$ is the 3x3 rotation matrix and $\boldsymbol{p}_n^v$ is the position vector from frame Ψ_v to Ψ_n. The spring $\boldsymbol{K} \in \mathbb{R}^{6x6}$ is described by a positive definite, symmetric matrix:

$$\boldsymbol{K} = \begin{pmatrix} \boldsymbol{K}_{\mathrm{o}} & \boldsymbol{K}_{\mathrm{c}} \\ \boldsymbol{K}_{\mathrm{c}} & \boldsymbol{K}_{\mathrm{t}} \end{pmatrix}, \tag{3}$$

where $\boldsymbol{K}_{\mathrm{o}} \in \mathbb{R}^{3x3}$, $\boldsymbol{K}_{\mathrm{t}} \in \mathbb{R}^{3x3}$ and $\boldsymbol{K}_{\mathrm{c}} \in \mathbb{R}^{3x3}$ refer to the rotational, translational and coupling elements of the spring. The wrench, $\boldsymbol{W}_s^n = \begin{bmatrix}\tau_s^n & f_s^n\end{bmatrix}$, exerted by the spring on the end-effector is [21]:

$$\tilde{\boldsymbol{\tau}}^n = -2\mathrm{as}(\boldsymbol{G}_{\mathrm{o}}\boldsymbol{R}_n^v) - \mathrm{as}(\boldsymbol{G}_{\mathrm{t}}\boldsymbol{R}_v^n\tilde{\boldsymbol{p}}_n^v\tilde{\boldsymbol{p}}_n^v\boldsymbol{R}_n^v) - 2\mathrm{as}(\boldsymbol{G}_{\mathrm{c}}\tilde{\boldsymbol{p}}_n^v\boldsymbol{R}_n^v), \tag{4}$$

$$\tilde{\boldsymbol{f}}^n = -\boldsymbol{R}_v^n\mathrm{as}(\boldsymbol{G}_{\mathrm{t}}\tilde{\boldsymbol{p}}_n^v)\boldsymbol{R}_n^v - \mathrm{as}(\boldsymbol{G}_{\mathrm{t}}\boldsymbol{R}_v^n\tilde{\boldsymbol{p}}_n^v\boldsymbol{R}_n^v) - 2\mathrm{as}(\boldsymbol{G}_{\mathrm{c}}\boldsymbol{R}_n^v), \tag{5}$$

where the $\mathrm{as}(\cdot)$ operator gives the anti-symmetric part of a square matrix, the $\tilde{(\cdot)}$ operator the skew symmetric representation of a vector and

$$\boldsymbol{G}_\gamma = \frac{1}{2}\mathrm{tr}(\boldsymbol{K}_\gamma)\boldsymbol{I}_{3\times 3} - \boldsymbol{K}_\gamma, \tag{6}$$

with $\gamma \in \{\mathrm{c},\mathrm{o},\mathrm{t}\}$ and the $\mathrm{tr}()$ operator gives the trace of a square matrix. The wrench can be transformed to joint torques by taking the adjoint to express the wrench in the inertial frame:

$$(\boldsymbol{W}_s^0)^\top = \mathrm{Ad}_{\boldsymbol{H}_0^n}^\top(\boldsymbol{W}_s^n)^\top, \tag{7}$$

and subsequently transforming this wrench to joint torques via:

$$\boldsymbol{\tau}^\top = \boldsymbol{J}^\top(\boldsymbol{q})(\boldsymbol{W}_s^0)^\top, \tag{8}$$

where $\boldsymbol{J}(\boldsymbol{q})$ is the geometric Jacobian of the manipulator.
The effect of the Cartesian damper can be described similarly. The damper $\boldsymbol{B}$ acts on the twist vector, a 6-dimensional column vector described as:

$$\boldsymbol{T}_{\boldsymbol{a}}^{\boldsymbol{c,b}} = \begin{bmatrix}\boldsymbol{\omega}_a^{c,b} & \boldsymbol{v}_a^{c,b}\end{bmatrix}, \tag{9}$$

where $\boldsymbol{\omega}$ and $\boldsymbol{v}$ denote the angular and linear velocity vectors. This twist's indices notation indicates the twist of frame *a* with respect to frame *b* expressed in frame *c*. The wrench exerted by the damper expressed in Ψ_n is described as:

$$\boldsymbol{W}_d^n = \boldsymbol{B}\boldsymbol{T}_n^{n,0}, \tag{10}$$

where $\boldsymbol{B} \in \mathbb{R}^{6x6}$ denotes the positive definite damping matrix. This wrench is transformed to joint torques via (7) and (8). Finally, the actuator torques are expressed as:

$$\boldsymbol{\tau}^\top = \boldsymbol{J}^\top(\boldsymbol{q})(\boldsymbol{W}_s^0 + \boldsymbol{W}_d^0)^\top. \tag{11}$$

III. Control Strategy

The work as shown in this section is based on previous work presented in [18]. For completeness the main concepts are repeated in this section. However, it should be noted that we made two changes regarding the control strategy:

1) High jerk motions are difficult to realise on the real system. Therefore, the cost function is augmented by a term that penalises high jerk.
2) Since the manipulator used for validation is a redundant robot, we choose a joint space impedance controller

for the task-free term as opposed to a Cartesian space impedance controller.

An overview of the control architecture can be found in Fig. 3. The control torque is split in a task-free term τ_{TF}

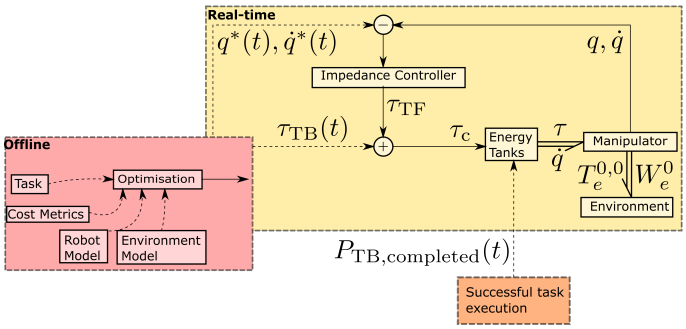

Fig. 3: The control architecture with the task-based and task-free controllers. The dashed lines represent signals computed offline, while the solid lines show signals computed in real-time.

and a task-based term τ_{TB}. The combination of a task-based and a task-free term allows to use only minor feedback, resembling a biomimetic approach [19, 22, 23]. We briefly motivate the control architecture here, before explaining the details in Section III-A to Section IV. The task-based control action comprises a feed-forward torque $\boldsymbol{\tau}_{\mathrm{TB}}(t)$ constructed by an offline optimisation algorithm based on gradient descend. It is constructed using time-varying values for the impedance parameters $\boldsymbol{K}$ and $\boldsymbol{B}$ in a Cartesian impedance control framework (Section II), and optimised with the task, cost metrics, and robot and environment models as input. We use the Cartesian impedance control framework such that:

1) The control action is physically interpretable. This gives an intuitive understanding of the optimisation results as shown in Section VI.
2) Given a fixed and reachable desired frame, the system is guaranteed to converge to that location for any positive stiffness values in nominal conditions. This increases the convergence rate compared to blind parametrisation of the joint torques.

Besides the feed-forward torques, the optimisation yields the nominal joint angles $\boldsymbol{q}^*(t)$ and joint velocities $\dot{\boldsymbol{q}}^*(t)$, which are used by the task-free impedance controller. The task-free joint impedance feedback term τ_{TF} compensates for disturbances from the nominal trajectory (Section III-B). Subsequently, the control torque $\boldsymbol{\tau}_{\mathrm{c}}$ is given by:

$$\boldsymbol{\tau}_{\mathrm{c}}(t, \boldsymbol{q}, \dot{\boldsymbol{q}}) = \boldsymbol{\tau}_{\mathrm{TB}}(t) + \boldsymbol{\tau}_{\mathrm{TF}}(\boldsymbol{q}, \dot{\boldsymbol{q}}) \tag{12}$$

Lastly, the control is made safe using energy tanks, augmented with a novel energy budgeting protocol (Section IV).

A. Task-Based optimisation

An optimal task-based control torque is found based on a biomimetic metric. We take inspiration from [22], suggesting that the human Central Nervous System (CNS) tries to minimise the metabolic cost while simultaneously minimising the motion error. We first define the to be optimised control torque as:

$$\boldsymbol{\tau} = \boldsymbol{J}(\boldsymbol{q})^\top \boldsymbol{W}^0 + \hat{\boldsymbol{G}}(\boldsymbol{q}), \tag{13}$$

where $\boldsymbol{W}^0$ is dependent on $\boldsymbol{K}$ and $\boldsymbol{B}$ from Eq. (7) and Eq. (10). The optimal solution is found by varying $\boldsymbol{K}$ over time to get a minimisation of the total cost:

$$\boldsymbol{K}(t)^* = \underset{\boldsymbol{K}(t)}{\operatorname{argmin}} J_{\mathrm{t}}. \tag{14}$$

The Cartesian stiffness $\boldsymbol{K}(t)$ is chosen to be diagonal. We optimise the the rotational, planar and vertical components of the stiffness matrix independently:

$$\boldsymbol{K}(t) = \mathrm{diag}(k_{\mathrm{o}}(t)\boldsymbol{I}_{3\times3}, k_{\mathrm{p}}(t)\boldsymbol{I}_{2\times2}, k_{\mathrm{v}}(t)). \tag{15}$$

The damping coefficients in $\boldsymbol{B}(t)$ directly depend on the stiffness coefficients:

$$b_\gamma = 2\sqrt{k_\gamma m}, \tag{16}$$

with $\gamma \in \{\mathrm{o}, \mathrm{p}, \mathrm{v}\}$ and $m \in \mathbb{R}_+$. m is chosen based on the upper bound of the inertia matrix, for a detailed explanation on the coefficient m we refer to [24]. Since the optimisation problem as stated in Eq. (14) is of infinite-dimensional nature i.e. the decision variable $\boldsymbol{K}$ is a vector valued function of time, we reduce the amount of optimisation variables by formulating the stiffness curves as uniformly distributed B-splines:

$$k_\gamma(t) = \sum_{i=1}^{N_{\mathrm{coefs}}} \alpha_{\gamma,i} S_i(t), \tag{17}$$

with N_{coefs} the amount of coefficients, $S_{\mathrm{i}}(t)$ are the spline basis functions and $\alpha_{\gamma,i}$ are the coefficients. The coefficients form the optimisation variables to be solved for, this reduces the optimisation variables to a finite set of $3N_{\mathrm{coefs}}$ variables. The optimisation problem becomes:

$$\boldsymbol{\alpha}^* = \underset{\alpha}{\operatorname{argmin}}\, J_{\mathrm{t}} \quad \text{s.t.} \quad k_\gamma^+ \geq k_\gamma(\boldsymbol{\alpha}_\gamma, t) \geq k_\gamma^- \quad \forall t. \tag{18}$$

When $\boldsymbol{\alpha}^*$ has been found the we compute the optimal task-based torque as:

$$\boldsymbol{\tau}_{\mathrm{TB}}(t) = \boldsymbol{J}(\boldsymbol{q}^*)^\top \boldsymbol{W}^0(\boldsymbol{\alpha}^*, \boldsymbol{q}^*, \dot{\boldsymbol{q}}^*) + \hat{\boldsymbol{G}}(\boldsymbol{q}^*). \tag{19}$$

In the next paragraphs it is outlined how J_{t} is constructed, with w_1, w_2, w_3, w_4 weighing constants.

1) Performance cost: The task performance is split between two terms $J_{\mathrm{p}} = J_{\mathrm{e}} + J_{\mathrm{j}}$. The first cost J_{e}, is the cost based on the absolute error for each desired robot pose:

$$J_{\mathrm{e}} = w_1 ||\boldsymbol{H}_n^v(T) - \boldsymbol{I}_4||^2_{\mathrm{FRO}}, \tag{20}$$

where T are the the final time instances of the multi-phase trajectory. Contrary to [18] we add a second term that minimises the jerk, as the real system cannot track rapidly varying torque references:

$$J_{\mathrm{j}} = w_2 \sum_{j=1}^{N_{\mathrm{joints}}} \int_0^T |\dddot{q}_j| dt. \tag{21}$$

2) Metabolic cost: The metabolic cost comprises the energy spent during the task. This consists of the electrical resistance loss in the electrical domain and the power output to the mechanical domain. The electrical resistance loss is described by:

$$P_{\mathrm{e}} = \sum_{\mathrm{j}=1}^{N} i_j^2 R_j = \sum_{\mathrm{j}=1}^{N_{\mathrm{joints}}} C \cdot \tau_{\mathrm{c},j}^2, \tag{22}$$

with N the number of joints and C being the approximated electrical resistance losses. The mechanical power output is described by:

$$P_{\mathrm{m}} = \boldsymbol{\tau}_{\mathrm{c}} \dot{\boldsymbol{q}}. \tag{23}$$

It is assumed that the motors do not have four-quadrant control capabilities, hence we take the absolute value of the mechanical power output. Subsequently, the total metabolic cost can be defined as:

$$J_{\mathrm{m}} = w_3 \int_0^T P_{\mathrm{e}} + (P_{\mathrm{m}})^+ dt, \tag{24}$$

where $(\cdot)^+$ denotes the positive part of the argument.

3) Stiffness cost: The last term penalises high stiffness of the Cartesian spring. For safety reasons it is recommended to use the lowest stiffness possible to complete the task, such that the interaction energy is minimised. Additionally, using the optimisation parameters directly in the objective function provides regularisation to the optimisation procedure. The stiffness cost can be defined as a function of the direct optimisation variable:

$$J_{\mathrm{k}} = w_4 \boldsymbol{\alpha}^\top \boldsymbol{\alpha}. \tag{25}$$

B. Task-Free control

We add a feedback control term to the feedforward term to account for model uncertainties and external disturbances, we call this the task-free term. The task-free controller is defined as a joint-space impedance controller:

$$\boldsymbol{\tau}_{\mathrm{TF}} = \boldsymbol{K}_{\mathrm{TF}}(\boldsymbol{q}^* - \boldsymbol{q}) + \boldsymbol{B}_{\mathrm{TF}}(\dot{\boldsymbol{q}}^* - \dot{\boldsymbol{q}}), \tag{26}$$

with $\boldsymbol{K}_{\mathrm{TF}} \in \mathbb{R}^{N\times N}$, $\boldsymbol{B}_{\mathrm{TF}} \in \mathbb{R}^{N\times N}$, and $\boldsymbol{q}^*$ and $\dot{\boldsymbol{q}}^*$ resulting from the optimisation procedure.

IV. Safety Layer

In this work we focus on post-impact safety. Safety after impact, or after an unexpected collision has occurred, consists of a collision detection and a collision reaction part. In this framework the collision detection strategy is formulated by exploiting the energy tank architecture. Stability of systems interacting with unknown (passive) environments can be guaranteed by means of passivity of the controlled system [25]. However, to perform a task, the controlled system may need to vary the virtual reference frame and, with variable impedance, the stiffness of the control spring. These variations generate power ports, injecting energy into the system and destroying passivity. On top of that, real world tasks often requires the robot to perform active work on the environment. Energy tanks are an elegant way of recovering passivity and can be readily applied on multi-DoF manipulators [12].

A. Energy Tanks

Energy tanks can represented by physical energy storage elements, e.g. a spring or capacitor, connected to each joint. In this work, the energy tanks are modelled as mechanical springs, which potential energy is described by:

$$H_j(d_j) = \frac{1}{2} d_j^2, \tag{27}$$

for the tank in joint j, where d_j is the tank state (spring deflection) and stiffness is unity. The dynamic equation describing the interconnection of the energy tanks with the manipulator is described by:

$$\begin{pmatrix} \dot{d}_j \\ \tau_{\mathrm{o},j} \end{pmatrix} = \begin{pmatrix} 0 & u_j \\ -u_j & 0 \end{pmatrix} \begin{pmatrix} d_j \\ \dot{q}_j \end{pmatrix} + \begin{pmatrix} 1 \\ 0 \end{pmatrix} U_j, \tag{28}$$

where d_j are the states of the energy tanks, $\tau_{\mathrm{o},j}$ are the output torques, $\dot{q}_j$ are the joint velocities and U_j is used to inject energy into the energy tanks. Fig. 4 shows an actuator joint connected to a tank subsystem. Each actuator can draw energy from its corresponding tank through a modulated transformer (MTF) with transformation ratio u_j:

$$u_j = -\frac{\tau_{\mathrm{c},j}}{d_j}, \tag{29}$$

under nominal conditions, where $\tau_{\mathrm{c},j}$ is the control torque for each joint. $\boldsymbol{\tau}_{\mathrm{c}}$ is not a passive control action due to the feedforward term in Eq. (12) in the task-based part, and due to the time dependence of the joint and velocity reference in the task-free part. We can recover passivity by setting $U_j = 0$ and by decoupling the energy tanks from the actuators, i.e. $u_j = 0$, in case the energy in one of the tanks has exceeded its preset energy limits.

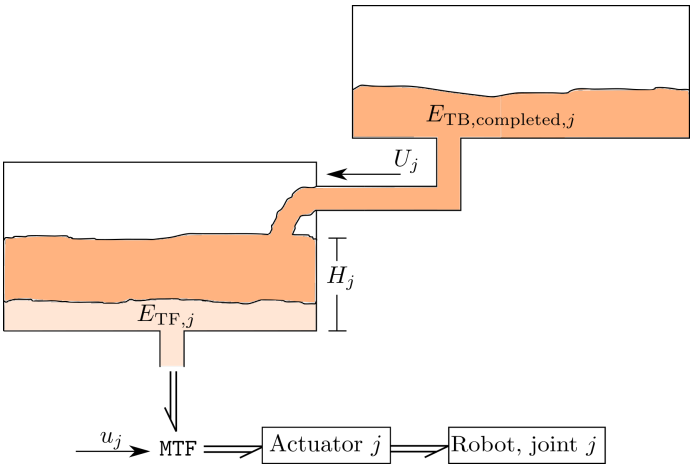

Fig. 4: Schematic tank subsystem of joint j. The modulated transformer (MTF) modulates the power flow between tank and actuator by means of ratio u_j.

B. Dynamic Energy Injection

In the previous section and in other works energy tanks are used to recover passivity, usually under the guise of safety. However, one substantial issue with this approach is that the content of the energy tank can render the system unsafe, despite the system being passive. We solve this by using a novel dynamic energy injection protocol, which fits very well within the task-based paradigm. From the nominal task the total energy consumption can be derived, which can be used to set the energy stored in the tank at the beginning of each task. This is called the task-based energy E_{TB}, which can be computed offline via $E_{\mathrm{TB}} = \int_0^T P_{\mathrm{TB}} dt$, where $P_{\mathrm{TB}}(t) = \boldsymbol{\tau}_{\mathrm{TB}}(t)\dot{\boldsymbol{q}}^*(t)$. Since the actual task will differ from the nominal task, we add an energy margin called the task-free energy E_{TF}. The initial energy in the tank is set by the task-free energy:

$$d_j(0) = \sqrt{2E_{\mathrm{TF},j}}. \tag{30}$$

This strategy showed promising results [18]. However, despite using the well-identified model from [26], there exists a significant discrepancy between the mechanical power as expected by the optimisation and the mechanical power measured on the real system. To solve this issue we use a new task-based power for dynamic energy injection, which uses measurement data from a successfully completed task:

$$P_{\mathrm{TB,completed}}(t) = \boldsymbol{\tau}_{\mathrm{measured}}(t)\dot{\boldsymbol{q}}_{\mathrm{measured}}(t), \tag{31}$$

so it is necessary to first perform the task on the real system before being able to use the safety layer. This is illustrated in Fig. 3. We choose to dynamically inject the task-based energy, such that the energy content within the tanks is as low as possible. Hence, the energy content in the tanks is set by:

$$d_j(0) = 2 \cdot \sqrt{E_{\mathrm{TF},j}}, \quad U_j(t) = \frac{P_{\mathrm{TB,completed},j}(t)}{d_j}. \tag{32}$$

By using this strategy the system will be non-passive, but much safer compared to the conventional passive approach, since the total energy of the system is guaranteed lower. This approach might seem a bit paradoxical since we wittingly renounce to passivity, which is the reason why normally energy tanks are introduced. Nevertheless, this is an effective way to use this architecture for guaranteeing safety, which should be the main motivation for introducing such energy-aware control layer.

C. Collision detection and reaction

By using the dynamic energy injection protocol with the energy tanks, we can detect if anything unexpected occurs. A collision has been detected when the energy in the tank has deviated significantly from its starting position. One advantage of the chosen strategy is that we can still perform an interaction task (planned collision) if the interaction task is consistent between iterations.

In case an unplanned collision occurs, a two-phase reaction strategy is proposed:

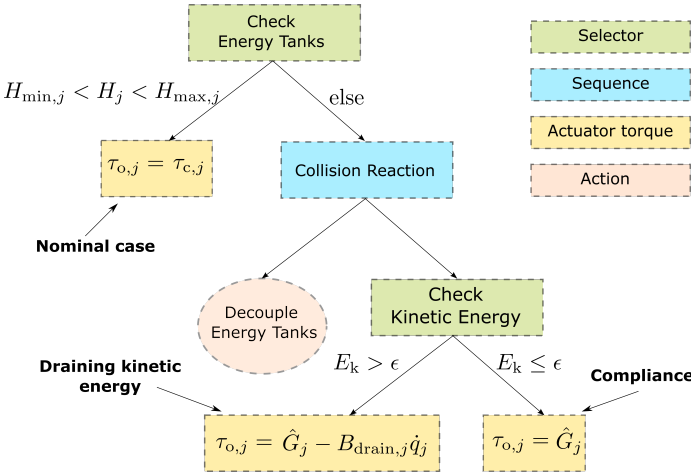

Fig. 5: Behaviour tree for regulating the actuator torques.

1) Kinetic energy is removed from the system. This is done by setting a high damping, B_{drain}, on the joint velocities and combining this with a gravity compensation term to prevent acceleration due to gravity.
2) After the kinetic energy has been removed, the system becomes compliant, such that the robot can be removed from the collided object with minimum effort. Hence, the control torques in this phase only consist of the gravity compensation term.

This strategy is visualised in the behaviour tree in Fig. 5. We have two selectors, the first one at the top of the figure checks the energy tanks content. If the content in each of the energy tanks is not too high or too low we set the actuator torque as $\tau_{c,j}$, i.e. we set the transformation ratio as in Eq. (29), such that the task-based and task-free control torques are send to the actuators. If this is not the case we follow a sequence:

1) Decouple the energy tanks, i.e. $u_j = 0$ and $U_j = 0$.
2) The selector determines whether or not to drain the energy or become compliant depending on the total kinetic energy of the system.

V. Experiment Setup

A. Hardware

1) Franka: To validate the proposed control architecture, a peg-in-hole experiment was conducted on a real robotic-platform, using the Franka Emika Panda robotic arm. The Franka Control Interface (FCI) is commanded via the Robotic Operating System (ROS).

2) Task: We perform a peg-in-hole task, as it is a benchmark test in industrial robotics. The peg is placed on a stand with a known location. The first phase of the task will consist of grabbing the peg with sufficient accuracy. Secondly, the peg is brought above the hole location and subsequently inserted in the hole in which a compression spring is placed. The final task is to compress the spring up to a certain distance. For a visualisation of the task we refer to Fig. 1 and Fig. 7.

B. Software

1) Nodes: Two ROS nodes are required to be able to execute the peg-in-hole task; one for controlling the joint torques, called the `control_node` and one for controlling the gripper for grabbing/releasing the peg, called the `gripper_node`. A schematic overview of the communication between nodes and hardware can be found in Fig. 6. The `control_node` publishes a flag on a certain topic to which the `gripper_node` is subscribed. This way the gripper knows when to perform a grabbing or releasing action.

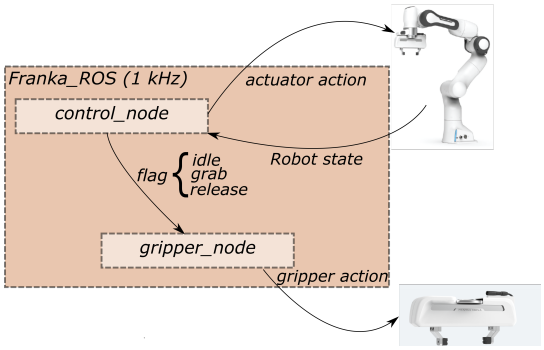

Fig. 6: Communication between ROS nodes and hardware.

2) Trajectory: The peg-in-hole task requires the end-effector to follow a set of poses from a certain starting configuration, taking into account constraints of the hardware. Fig. 7 shows the end-effector poses required to complete the task. The trajectory is constructed by solving the dynamic equations using Matlab's `ode15s` solver. We solve for each pose consecutively i.e. once a pose has been reached we change the virtual reference frame Ψ_v and solve for the new pose.

3) Optimisation to FCI: The optimisation to FCI interface is depicted in Fig. 8. The optimisation outputs from Matlab are loaded into the `C++` script. A joint space impedance controller brings the manipulator to the correct initial position. Subsequently, the control strategy from Section III and Section IV is followed, which results in the output torque commands τ_o that can be send to the FCI.

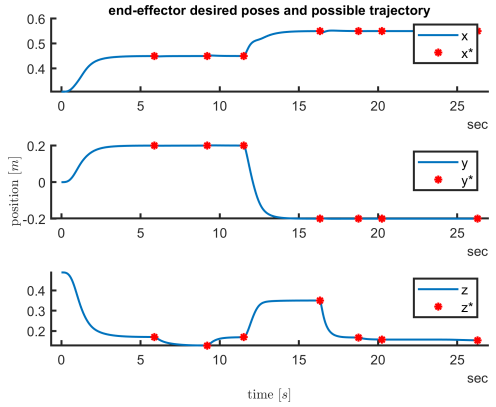

Fig. 7: The desired poses of the end-effector (red star) and a possible trajectory that completes the poses (blue line).

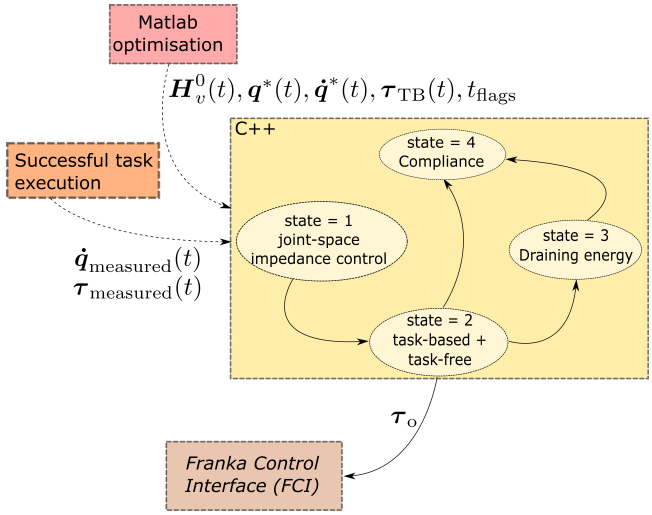

Fig. 8: Workflow from Matlab optimisation to FCI. Solid lines are offline signals, while dashed lines are real-time signals at 1 kHz.

VI. Results

To obtain the relevant data we run the optimisation algorithm with the parameters as given in Table I. We validate our approach in two steps:

1) We execute the task without any unplanned activities. This is done multiple times to check for reliability of the control scheme and the sensitivity of the safety layer. Additionally, we investigate the effectiveness of the open-loop control torques.
2) We collide the manipulator with a human test subject to test sensitivity of the collision detection and the compliance of the reaction strategy.

The experiments have been performed with the parameters as given in Table II, where k_{spring} is the spring constant of the compression spring used for the compression task and $k_{\text{TF,max}}$ is the maximum value for each entry of the feedback gain $\boldsymbol{K}_{\text{TF}}$. Additionally, we keep the internal Franka collision detection turned on during the experiments. Since our collision

parameter	value	unit
w_1	1e6	-
w_2	5e-6	-
w_3	0.1	-
w_4	1e-8	-
T_{final}	30	[s]
N_{coefs}	30	-
C	0.0082	$[\text{N}^{-1}\,\text{m}^{-1}\,\text{s}^{-1}]$
k_γ^-	20	$[\text{N}\,\text{m}^{-1}]$
k_γ^+	1e5	$[\text{N}\,\text{m}^{-1}]$

TABLE I: Parameters for the optimisation problem.

parameter	value	unit
k_{TF}	100	$[\mathrm{N\,m\,rad^{-1}}]$
$k_{\mathrm{TF,max}}$	400	$[\mathrm{N\,m\,rad^{-1}}]$
k_{spring}	5240	$[\mathrm{N\,m^{-1}}]$
b_{TF}	15	$[\mathrm{N\,m\,s\,rad^{-1}}]$
b_{drain}	40	$[\mathrm{N\,m\,s\,rad^{-1}}]$

TABLE II: Parameters used in the experiments on the Franka Emika Panda manipulator.

detection protocol is able to use information of the task, our collision detection should at the minimum be more sensitive than the internal collision detection of the Franka.

A. Executing the task without collisions

1) Effectiveness of the open-loop torques: Fig. 9 show the task-based and task-free torques over time and in Fig. 10 the tracking of the joint angles is shown. A key observation to make here is the task-free torques partly cancelling the task-based torques. This shows that there is a discrepancy between the nominal case and the real system. This discrepancy can be partly attributed to imperfections in the manipulator model. However, another reason for this discrepancy is that we are changing the reference frame, while the stiffness of the control spring is non-zero $k_\gamma \neq 0$. This introduces a step function in the control torques, which the real manipulator is not able to track. This problem could be solved by putting additional constraints on the behaviour of k_γ in the optimisation step. Nevertheless, the task-based torques do contribute to the robot motion for the parts that are not cancelled by the task-free control action.

2) Effectiveness of the safety layer: Fig. 11 shows the energy contents in the tanks while performing the task. The limits in the tanks are chosen differently for each joint. The second and the fourth joint have to provide the most power to complete the task, which correlates to bigger discrepancies between power transferred for each task. Two key points of interest can be extracted from the figure:

1) We are sensing a deviation from the nominal task, as the dynamic energy injection is not perfect i.e. the energy in the tanks is not constant. However, these deviations are not significant enough to be labelled a collision. Hence, the task can be performed consistently, even though the energy bounds in the tanks are relatively narrow. The task was repeated five times in a row without any interventions from the safety layer, which shows that the safety layer is not too sensitive
2) From $t = 23.5\,\mathrm{s}$ it can be concluded that the interaction task does not produce a significant deviation in the energy tanks. This is due to the relatively simple and consistent interaction environment, which enables us to keep the energy limits of the tanks constant throughout the entire trajectory. In case the interaction environment deviates significantly between iterations, the bounds can be relaxed during that part of the trajectory, since the manipulator velocities are low and thus the robot is relatively safe.

B. Executing the task while colliding with a human

Fig. 12 shows the energy contents in the tanks while performing the task. From the figure it can be concluded that joint 2 is empty around $200\,\mathrm{ms}$ after the collision occurred. Fig. 13 shows the end-effector trajectory. After a few seconds the user is interacting with the manipulator to test the compliance off the robot. The user reported that the robot could be moved around with minimal effort. We like to refer to the supplementary material[1] for the video recordings of these experiments. Additionally, in the supplementary material there are also collision experiments presented with a collision towards the end of the trajectory. In this case the energy tanks have already diverged from their starting value, but the sensitivity of the collision detection did not experience a significant decline.

C. Results discussion

In the experiments as shown in Section VI-B the internal collision detection of the Franka manipulator was not triggered. This shows the effectiveness of our proposed strategy. Although the safety layer did not intervene during the experiments from Section VI-A, it should be noted that outside of these experiments the safety layer unnecessarily intervened a few times. Mostly, when the robot has been turned off for a long time. This can be prevented by either dynamically adjusting the bounds or increasing the energy tank thresholds.

VII. Conclusion

We have proposed an energy-and safety-aware control strategy that incorporates the task-based nature of the control scheme in the energy-tank architecture. The energy-tanks were utilised using a dynamic energy injection protocol, which destroys passivity, but provides the system with a post-impact safety layer. The proposed strategy was experimentally validated with the Franka Emika Panda 7-DoF manipulator. Experiments with free motion and obstructed motion show that the safety layer is both sensitive and reliable. This can be partly shown with the lack of collision detection by the internal Franka safety layer. Pre-impact safety is incorporated in the cost function of the optimisation algorithm, but for future work we propose to extend this by incorporating pre-impact safety limits in terms of impact force or energy transfer as optimisation constraints to ensure complete safety of the manipulator.

[1] https://cloud.ram.eemcs.utwente.nl/index.php/s/5bzLDEqwQqANKeE

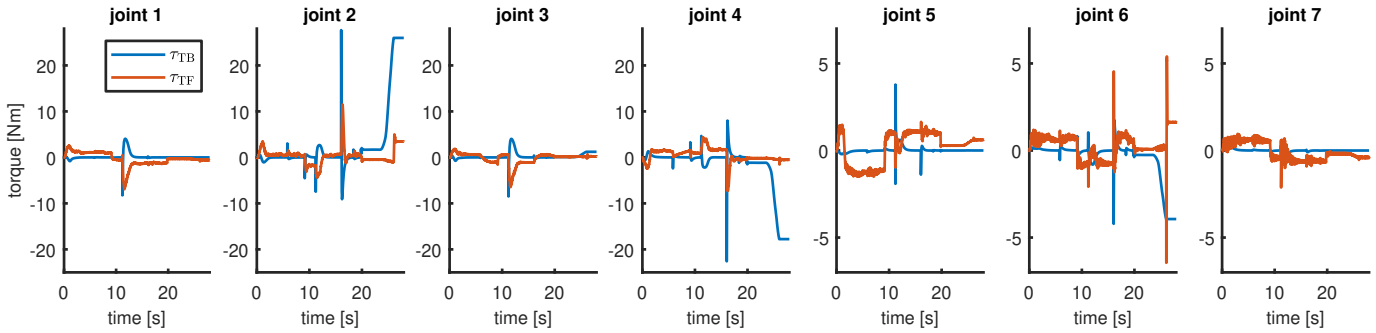

Fig. 9: Experiment without collision: The task-based and task-free torques for each joint for a successful completion of the task. Data corresponding to experiment 4 in the supplementary material.

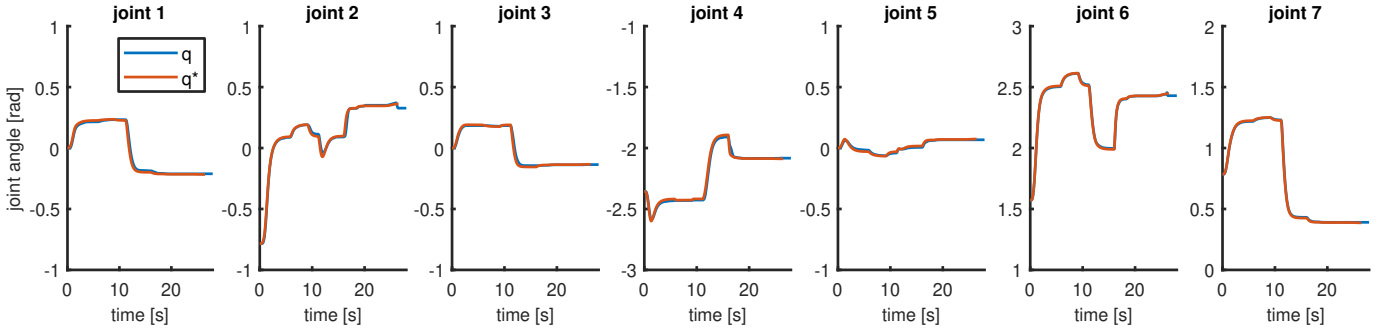

Fig. 10: Experiment without collision: the reference joint angles q^* and the measured joint angles q. Data corresponding to experiment 4 in the supplementary material.

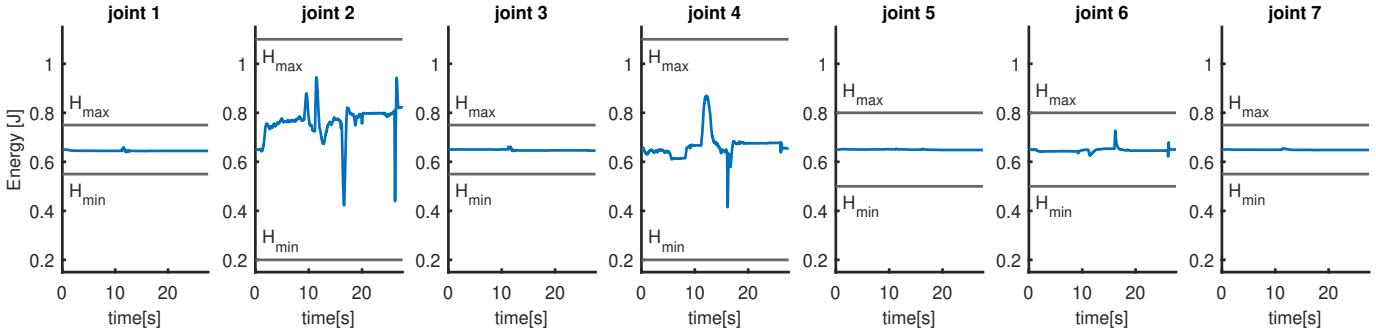

Fig. 11: Experiment without collision: Energy levels of the tanks in each joint. The initial energy in each tank is arbitrarily chosen at $0.65\,\mathrm{J}$. Blue lines represent the energy levels in the tank, while the black horizontal lines represent the energy limits for each tank. Data corresponding to experiment 4 in the supplementary material.

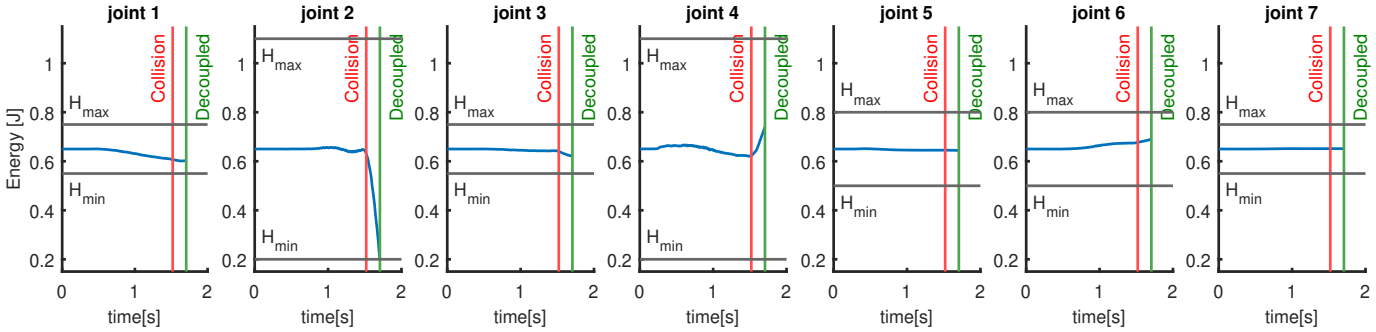

Fig. 12: Experiment with human-robot collision: Energy levels of the tanks in each joint. Vertical red and green lines show the instances of collision and decoupling respectively. Data corresponding to experiment 15 in the supplementary material.

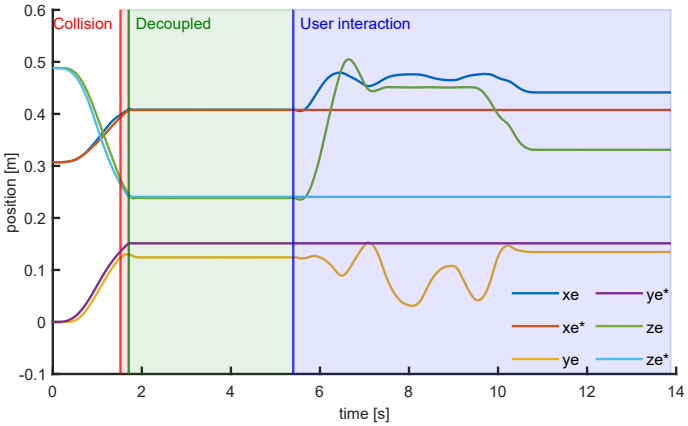

Fig. 13: Experiment with human-robot collision: End-effector position along the trajectory. Vertical red and green liens show the instances of collision and decoupling respectively. The blue vertical line shows when the human is interacting with the manipulator freely. Data corresponding to experiment 15 in the supplementary material.

References

[1] J.Edward Colgate, Witaya Wannasuphoprasit, and Michael A. Peshkin. "Cobots: robots for collaboration with human operators". In: vol. 58. 1996, pp. 433–439.

[2] Sami Haddadin and Elizabeth Croft. "Physical Human–Robot Interaction". In: *Springer Handbook of Robotics*. Ed. by Bruno Siciliano and Oussama Khatib. Cham: Springer International Publishing, 2016, pp. 1835–1874. ISBN: 978-3-319-32552-1. DOI: 10.1007/978-3-319-32552-1_69.

[3] Lucia Pigini et al. "Service robots in elderly care at home: Users' needs and perceptions as a basis for concept development". In: *Technology and Disability* 24 (Dec. 2012), pp. 303–311. DOI: 10.3233/TAD-120361.

[4] Y. Yamada et al. "FTA-based issues on securing human safety in a human/robot coexistence system". In: *IEEE SMC'99 Conference Proceedings. 1999 IEEE International Conference on Systems, Man, and Cybernetics (Cat. No.99CH37028)*. Vol. 2. 1999, 1058–1063 vol.2. DOI: 10.1109/ICSMC.1999.825409.

[5] R. Schiavi, A. Bicchi, and F. Flacco. "Integration of active and passive compliance control for safe human-robot coexistence". In: 2009, pp. 259–264. DOI: 10.1109/ROBOT.2009.5152571.

[6] Albert-Jan Baerveldt. "A safety system for close interaction between man and robot". In: *Safety of Computer Control Systems 1992 (Safecomp ' 92)*. Ed. by Heinz H. Frey. IFAC Symposia Series. Oxford: Pergamon, 1992, pp. 25–29. ISBN: 978-0-08-041893-3. DOI: https://doi.org/10.1016/B978-0-08-041893-3.50009-4.

[7] Dana Kulic and Elizabeth Croft. "Pre-collision safety strategies for human-robot interaction". In: *Auton. Robots* 22 (Jan. 2007), pp. 149–164. DOI: 10.1007/s10514-006-9009-4.

[8] Ravinder S. Dahiya et al. "Directions Toward Effective Utilization of Tactile Skin: A Review". In: *IEEE Sensors Journal* 13.11 (2013), pp. 4121–4138. DOI: 10.1109/JSEN.2013.2279056.

[9] K. Suita et al. "A failure-to-safety "Kyozon" system with simple contact detection and stop capabilities for safe human-autonomous robot coexistence". In: *Proceedings of 1995 IEEE International Conference on Robotics and Automation*. Vol. 3. 1995, 3089–3096 vol.3. DOI: 10.1109/ROBOT.1995.525724.

[10] S. Takakura, T. Murakami, and K. Ohnishi. "An approach to collision detection and recovery motion in industrial robot". In: *15th Annual Conference of IEEE Industrial Electronics Society*. 1989, 421–426 vol.2. DOI: 10.1109/IECON.1989.69669.

[11] J. Heinzmann and A. Zelinsky. "Quantitative safety guarantees for physical human-robot interaction". In: *International Journal of Robotics Research* 22.7-8 SPECIAL ISSUE (2003), pp. 479–504. DOI: 10.1177/027836403128965231.

[12] G. Raiola et al. "Development of a Safety- and Energy-Aware Impedance Controller for Collaborative Robots". In: *IEEE Robotics and Automation Letters* 3.2 (2018), pp. 1237–1244. DOI: 10.1109/LRA.2018.2795639.

[13] R. Rossi et al. "A pre-collision control strategy for human-robot interaction based on dissipated energy in potential inelastic impacts". In: *2015 IEEE/RSJ International Conference on Intelligent Robots and Systems (IROS)*. 2015, pp. 26–31. DOI: 10.1109/IROS.2015.7353110.

[14] W. Roozing, S.S. Groothuis, and S. Stramigioli. "Energy-based Safety in Series Elastic Actuation". In: 2020, pp. 914–920. DOI: 10.1109/ICRA40945.2020.9197448.

[15] T. S. Tadele, T. J. A. de Vries, and S. Stramigioli. "Combining energy and power based safety metrics in controller design for domestic robots". In: *2014 IEEE International Conference on Robotics and Automation (ICRA)*. 2014, pp. 1209–1214. DOI: 10.1109/ICRA.2014.6907007.

[16] M. Laffranchi, N.G. Tsagarakis, and D.G. Caldwell. "Safe human robot interaction via energy regulation control". In: 2009, pp. 35–41. DOI: 10.1109/IROS.2009.5354803.

[17] N. Mansfeld et al. "Safety Map: A Unified Representation for Biomechanics Impact Data and Robot Instantaneous Dynamic Properties". In: *IEEE Robotics and Automation Letters* 3.3 (2018), pp. 1880–1887. DOI: 10.1109/LRA.2018.2801477.

[18] B. Gerlagh et al. "Energy-aware adaptive impedance control using offline task-based optimization". In: *International Conference on Advanced Robotics, ICAR 2021* (2020).

[19] C. Della Santina et al. “Controlling Soft Robots: Balancing Feedback and Feedforward Elements”. In: *IEEE Robotics and Automation Magazine* 24.3 (2017), pp. 75–83. DOI: 10.1109/MRA.2016.2636360.

[20] Stefano Stramigioli. *Modern Robotics lecture notes*. University of Twente. 2019.

[21] Stefano Stramigioli. *Modeling and IPC Control of Interactive Mechanical Systems: A Coordinate-free Approach*. Undefined. Lecture Notes in Control and Information Sciences 266. Editors: M. Thoma, M. Morari. Springer, 2001. ISBN: 1-85233-395-2.

[22] C. Yang et al. “Human-like adaptation of force and impedance in stable and unstable interactions”. In: *IEEE Transactions on Robotics* 27.5 (2011), pp. 918–930. DOI: 10.1109/TRO.2011.2158251.

[23] E. Burdet et al. “The central nervous system stabilizes unstable dynamics by learning optimal impedance”. In: *Nature* 414.6862 (2001), pp. 446–449. DOI: 10.1038/35106566.

[24] Tadele Shiferaw Tadele. “Human-friendly robotic manipulators: safety and performance issues in controller design”. In: (). DOI: 10.3990/1.9789036537841.

[25] S. Stramigioli. “Energy-Aware robotics”. In: *Lecture Notes in Control and Information Sciences* 461 (2015). cited By 18, pp. 37–50. DOI: 10.1007/978-3-319-20988-3_3.

[26] C. Gaz et al. “Dynamic identification of the Franka Emika Panda Robot with retrieval of feasible parameters using penalty-based optimization”. In: *IEEE Robotics and Automation Letters* 4.4 (2019), pp. 4147–4154. DOI: 10.1109/LRA.2019.2931248.

4 Reflection

This chapter reflects on the work done during this graduation project. We briefly discuss the problems encountered and mistakes made during the project. After that, a final conclusion regarding the research questions posed in the introductory chapter is made. Additionally, some recommendations are made for future work.

4.1 Discussion

There are two events in my graduation project, which influenced the outcome of the project significantly:

1. The experimental setup has been changed relatively often. This could have been prevented with a more thorough risk assessment of the experiments. Due to the lack of detail in the experiment plan some delays have occurred that could have been prevented. The most significant delays were caused by:
   - Peg design: Initially, the peg had a smooth surface, such that it could be easily grabbed. However, the amount of force the peg had to exert on the environment was quite significant. Therefore, the peg needed to be grabbed such that the gripper could not slip from the peg requiring significant changes to the design.
   - Accuracy: Since the robot gets no feed-back on the exact location of the hole in which the peg had to be inserted (only an assumed location) a very high accuracy was necessary to insert and grab the peg. Experiencing these issues, as opposed to assessing these risks beforehand, delayed the final experiments a significant amount of time. Accuracy issues were caused by vibration of the robot platform, alignment of the experiment platform with the manipulator platform, sensor noise and static friction.

2. Pre-impact safety was not properly investigated in the preparation. A case study was performed to test this, and the other key aspects of the graduation project, but this lacked detail. Due to this a critical aspect of pre-impact safety could not be understood, namely the effective mass. The limiting factors in pre-impact safety, i.e. impact force and transferred energy, are dependent on this effective mass. During the attempt to implement this when simulating the Franka robot, very unintuitive values came out of this effective mass. This made it possible for the Franka to behave very dangerously, while staying within the safe boundaries for impact force and transferred energy. Due to this it was decided to drop the pre-impact safety from the assignment. Hence, a small part of the thesis could not be completed satisfactory.

4.2 Conclusion

In Section 1.3.2 two research questions were formulated. In this section we will reflect on those research questions.

1. *"Is it achievable to implement the control strategy on a commonly used manipulator? Does it still have the same benefits over conventional control as shown in the simulation results?* It proved to be relatively easy to implement the control strategy of [1] under the condition that a dynamic model of the manipulator is available, the optimisation algorithm and manipulator control code can be found in the supplementary material[1]. The discrepancy between model and the real-system required some changes to be made in the control

[1] https://cloud.ram.eemcs.utwente.nl/index.php/s/9Rryznxedo7GRtr

architecture with respect to [1]. Due to discrepancy between model and the real system the task-free torques were quite significant, which mitigates the benefit from the task-based control action a bit. However, it was shown that the task-based torque did make a contribution to the control of the manipulator. Therefore, we can conclude that there is still a benefit of using this task-based control architecture, be it slightly worse than in simulation.

2. *"Is the control strategy presented safe for human-robot collaboration in a shared workspace? What steps are necessary to make the control strategy safe for humans and robots in a shared workspace?"*
   A small step has been made towards safe behaviour in case of robot interaction with the environment. A reliable and very sensitive collision detection and reaction strategy has been developed and experimentally validated. However, the total system cannot guarantee complete safety yet. To make this possible the optimisation step will have to take into consideration actual safety limits as constraints. There is already some work done on that in [20], which can be used to extend the optimisation algorithm with these safety criteria. Another concern is that the suitability of the task-based approach in case a human is involved in the task has not been tested yet. The irregularities that can occur in case of physical human-robot interaction might prove difficulty in the dynamic energy injection protocol.

4.3 Recommendation

- Only post-impact safety could be tested on the Franka manipulator. Therefore, a strong recommendation for future work is to extend the safety layer by also including pre-impact safety. This could be done by adjusting the optimisation algorithm with additional constraints on the safety relevant metrics such as energy, power or impact force. Combining this work with the work done in [20] should encompass the whole aspect of safety in a shared structured environment with humans and robots.
- The interaction task involved consisted of compressing a spring with $k = 5240\,\mathrm{N\,m^{-1}}$ for 10 mm. Hence, the interaction energy is only 0.262 J. This is in the same order of magnitude as the margins in the energy tanks. The proposed control strategy would be even more powerful if it was possible to show that we can perform interaction tasks that have a bigger interaction energy than the energy margins in the tanks. It was not possible to show this with the current setup due to limitations of the available compression springs and the force that can be exerted by the Franka manipulator.
- It was chosen to use Matlab's fmincon function to perform the optimisation algorithm, as this worked very well for the case-study and in previous work. However, as the system become more complex the speed became a serious problem with the optimisation running up to 40 hours before converging. For future work, it is recommended to look at the casadi optimisation software. Which has similar behaviour, but runs a lot faster.
- The actuator signals were not continuous in time, due to $k_\gamma \neq 0$ when switching the reference frame. Because of this, we had to deal with a discrepancy between the handling of the control torques on the real system and in the optimisation. Therefore, we recommend to make the actuator signals continuous in time. Perhaps if this is done it won't be necessary to do an initial supervised completion of the task.
- The cost function for the metabolic cost needs to be correctly implemented, such that it has some physical meaning. The cost function was implemented according to Eq. (22), (23) and (24) in the paper. However, it does not make sense to first sum the contributions of each joint and integrate after. In order to have the metabolic cost reflect the actual

energy consumption, the metabolic cost should have looked like:

$$J_{\mathrm{m}} = w_3 \sum_{\mathrm{j}=1}^{N} \int_0^T (P_{\mathrm{e},j} + P_{\mathrm{m},j})^+ \, dt \tag{4.1}$$

Due to the significant different results between Eq. (4.1) and the way the metabolic cost was constructed in the paper (Eq. (22)-(24)), the result presented in the paper cannot be considered optimal in terms of the intended metabolic cost.

Bibliography

[1] B. Gerlagh et al. “Energy-aware adaptive impedance control using offline task-based optimization”. In: *International Conference on Advanced Robotics, ICAR 2021* (2020).

[2] Lucia Pigini et al. “Service robots in elderly care at home: Users’ needs and perceptions as a basis for concept development”. In: *Technology and Disability* 24 (Dec. 2012), pp. 303–311. DOI: 10.3233/TAD-120361.

[3] Sami Haddadin and Elizabeth Croft. “Physical Human–Robot Interaction”. In: *Springer Handbook of Robotics*. Ed. by Bruno Siciliano and Oussama Khatib. Cham: Springer International Publishing, 2016, pp. 1835–1874. ISBN: 978-3-319-32552-1. DOI: 10.1007/978-3-319-32552-1_69.

[4] W. Roozing, S.S. Groothuis, and S. Stramigioli. “Energy-based Safety in Series Elastic Actuation”. In: 2020, pp. 914–920. DOI: 10.1109/ICRA40945.2020.9197448.

[5] L. Rozo et al. “Learning optimal controllers in human-robot cooperative transportation tasks with position and force constraints”. In: vol. 2015-December. 2015, pp. 1024–1030. DOI: 10.1109/IROS.2015.7353496.

[6] F. Ferraguti, C. Secchi, and C. Fantuzzi. “A tank-based approach to impedance control with variable stiffness”. In: cited By 74. 2013, pp. 4948–4953. DOI: 10.1109/ICRA.2013.6631284.

[7] C. Yang et al. “Human-like adaptation of force and impedance in stable and unstable interactions”. In: *IEEE Transactions on Robotics* 27.5 (2011), pp. 918–930. DOI: 10.1109/TRO.2011.2158251.

[8] N. Hogan. “Impedance control: An approach to manipulation: Part I-theory”. In: *Journal of Dynamic Systems, Measurement and Control, Transactions of the ASME* 107.1 (1985). cited By 1964, pp. 1–7. DOI: 10.1115/1.3140702.

[9] N. Hogan. “Impedance control: An approach to manipulation: Part II-implementation”. In: *Journal of Dynamic Systems, Measurement and Control, Transactions of the ASME* 107.1 (1985). cited By 458, pp. 8–16. DOI: 10.1115/1.3140713.

[10] N. Hogan. “Impedance control: An approach to manipulation: Part III-applications”. In: *Journal of Dynamic Systems, Measurement and Control, Transactions of the ASME* 107.1 (1985). cited By 268, pp. 17–24. DOI: 10.1115/1.3140701.

[11] Y. Yamada et al. “FTA-based issues on securing human safety in a human/robot coexistence system”. In: *IEEE SMC’99 Conference Proceedings. 1999 IEEE International Conference on Systems, Man, and Cybernetics (Cat. No.99CH37028)*. Vol. 2. 1999, 1058–1063 vol.2. DOI: 10.1109/ICSMC.1999.825409.

[12] R. Schiavi, A. Bicchi, and F. Flacco. “Integration of active and passive compliance control for safe human-robot coexistence”. In: 2009, pp. 259–264. DOI: 10.1109/ROBOT.2009.5152571.

[13] Albert-Jan Baerveldt. “A safety system for close interaction between man and robot”. In: *Safety of Computer Control Systems 1992 (Safecomp ’92)*. Ed. by Heinz H. Frey. IFAC Symposia Series. Oxford: Pergamon, 1992, pp. 25–29. ISBN: 978-0-08-041893-3. DOI: https://doi.org/10.1016/B978-0-08-041893-3.50009-4.

[14] Dana Kulic and Elizabeth Croft. “Pre-collision safety strategies for human-robot interaction”. In: *Auton. Robots* 22 (Jan. 2007), pp. 149–164. DOI: 10.1007/s10514-006-9009-4.

[15] J. Heinzmann and A. Zelinsky. “Quantitative safety guarantees for physical human-robot interaction”. In: *International Journal of Robotics Research* 22.7-8 SPECIAL ISSUE (2003), pp. 479–504. DOI: 10.1177/0278364903128965231.

[16] G. Raiola et al. “Development of a Safety- and Energy-Aware Impedance Controller for Collaborative Robots”. In: *IEEE Robotics and Automation Letters* 3.2 (2018), pp. 1237–1244. DOI: 10.1109/LRA.2018.2795639.

[17] R. Rossi et al. “A pre-collision control strategy for human-robot interaction based on dissipated energy in potential inelastic impacts”. In: *2015 IEEE/RSJ International Conference on Intelligent Robots and Systems (IROS)*. 2015, pp. 26–31. DOI: 10.1109/IROS.2015.7353110.

[18] T. S. Tadele, T. J. A. de Vries, and S. Stramigioli. “Combining energy and power based safety metrics in controller design for domestic robots”. In: *2014 IEEE International Conference on Robotics and Automation (ICRA)*. 2014, pp. 1209–1214. DOI: 10.1109/ICRA.2014.6907007.

[19] M. Laffranchi, N.G. Tsagarakis, and D.G. Caldwell. “Safe human robot interaction via energy regulation control”. In: 2009, pp. 35–41. DOI: 10.1109/IROS.2009.5354803.

[20] N. Mansfeld et al. “Safety Map: A Unified Representation for Biomechanics Impact Data and Robot Instantaneous Dynamic Properties”. In: *IEEE Robotics and Automation Letters* 3.3 (2018), pp. 1880–1887. DOI: 10.1109/LRA.2018.2801477.

[21] K. Suita et al. “A failure-to-safety "Kyozon" system with simple contact detection and stop capabilities for safe human-autonomous robot coexistence”. In: *Proceedings of 1995 IEEE International Conference on Robotics and Automation*. Vol. 3. 1995, 3089–3096 vol.3. DOI: 10.1109/ROBOT.1995.525724.

[22] S. Takakura, T. Murakami, and K. Ohnishi. “An approach to collision detection and recovery motion in industrial robot”. In: *15th Annual Conference of IEEE Industrial Electronics Society*. 1989, 421–426 vol.2. DOI: 10.1109/IECON.1989.69669.

[23] A. De Luca and R. Mattone. “Actuator failure detection and isolation using generalized momenta”. In: *2003 IEEE International Conference on Robotics and Automation (Cat. No.03CH37422)*. Vol. 1. 2003, 634–639 vol.1. DOI: 10.1109/ROBOT.2003.1241665.

[24] A. Dietrich et al. “Passive Hierarchical Impedance Control Via Energy Tanks”. In: *IEEE Robotics and Automation Letters* 2.2 (2017), pp. 522–529. DOI: 10.1109/LRA.2016.2645504.

[25] Alin Albu-Schäffer, Christian Ott, and Gerd Hirzinger. “A Unified Passivity-based Control Framework for Position, Torque and Impedance Control of Flexible Joint Robots”. In: *The International Journal of Robotics Research* 26.1 (2007), pp. 23–39. DOI: 10.1177/0278364907073776. eprint: https://doi.org/10.1177/0278364907073776.

[26] C. Della Santina et al. “Controlling Soft Robots: Balancing Feedback and Feedforward Elements”. In: *IEEE Robotics and Automation Magazine* 24.3 (2017), pp. 75–83. DOI: 10.1109/MRA.2016.2636360.

[27] S. Haddadin, A. Albu-Schäffer, and G. Hirzinger. “Safety analysis for a human-friendly manipulator”. In: *International Journal of Social Robotics* 2.3 (2010), pp. 235–252. DOI: 10.1007/s12369-010-0053-z.

[28] Richard F Edlich et al. “Principles of emergency wound management”. In: *Annals of Emergency Medicine* 17.12 (1988), pp. 1284–1302. ISSN: 0196-0644. DOI: https://doi.org/10.1016/S0196-0644(88)80354-8.

[29] Sami Haddadin, Alin Albu-Schäffer, and Gerd Hirzinger. “Requirements for Safe Robots: Measurements, Analysis and New Insights”. In: *The International Journal of Robotics Research* 28.11-12 (2009), pp. 1507–1527. DOI: 10.1177/0278364909343970. eprint: https://doi.org/10.1177/0278364909343970.

[30] J.A. Newman and N. Shewchenko. “A Proposed New Biomechanical Head Injury Assessment Function - The Maximum Power Index”. In: *SAE Technical Papers* 2000-November.November (2000). DOI: 10.4271/2000-01-SC16.

[31] Ravinder S. Dahiya et al. “Directions Toward Effective Utilization of Tactile Skin: A Review”. In: *IEEE Sensors Journal* 13.11 (2013), pp. 4121–4138. DOI: 10.1109/JSEN.2013.2279056.

[32] Sami Haddadin et al. “On making robots understand safety: Embedding injury knowledge into control”. In: *The International Journal of Robotics Research* 31.13 (2012), pp. 1578–1602. DOI: 10.1177/0278364912462256. eprint: https://doi.org/10.1177/0278364912462256.

[33] I.D. Walker. “Impact Configurations and Measures for Kinematically Redundant and Multiple Armed Robot Systems”. In: *IEEE Transactions on Robotics and Automation* 10.5 (1994), pp. 670–683. DOI: 10.1109/70.326571.

[34] S. Stramigioli. “Energy-Aware robotics”. In: *Lecture Notes in Control and Information Sciences* 461 (2015). cited By 18, pp. 37–50. DOI: 10.1007/978-3-319-20988-3_3.

[35] A. M. Zanchettin, B. Lacevic, and P. Rocco. “A novel passivity-based control law for safe human-robot coexistence”. In: *2012 IEEE/RSJ International Conference on Intelligent Robots and Systems*. 2012, pp. 2276–2281. DOI: 10.1109/IROS.2012.6385797.

[36] Gerrit A. Folkertsma and Stefano Stramigioli. “Energy in Robotics”. In: *Foundations and Trends® in Robotics* 6.3 (2017), pp. 140–210. ISSN: 1935-8253. DOI: 10.1561/2300000038.

[37] Pål Johan From, Jan Tommy Gravdahl, and Kristin Ytterstad Pettersen. “Properties of the Dynamic Equations in Matrix Form”. In: *Advances in Industrial Control*. Advances in Industrial Control, 2014, pp. 285–305. DOI: 10.1007/978-1-4471-5463-1_9.